The Absence of ABCA1 Decreases Soluble ApoE Levels but Does Not Diminish Amyloid Deposition in Two Murine Models of Alzheimer Disease*

Veronica Hirsch-Reinshagen[‡1], Luis F. Maia[‡§], Braydon L. Burgess[‡2], Jean-Francois Blain[¶3], Kathryn E. Naus[‡], Sean A. McIsaac[‡], Pamela F. Parkinson[‡], Jennifer Y. Chan[‡], Gavin H. Tansley[‡], Michael R. Hayden[∥4], Judes Poirier[¶5], William Van Nostrand[**6], and Cheryl L. Wellington[‡7]

From the ‡Department of Pathology and Laboratory Medicine, University of British Columbia, Vancouver, British Columbia V4Z 5H5, Canada, the §Department of Neurology, Hospital Geral de Santo Antonio 4099-001, Porto, Portugal, ¶McGill Centre for Studies in Aging, Montreal, Quebec H4H 1R3, Canada, ∥Centre for Molecular Medicine and Therapeutics, University of British Columbia, Vancouver, British Columbia V4Z 5H5, Canada, and the **Department of Medicine, Stony Brook University, Stony Brook, New York 11794

ABCA1, a cholesterol transporter expressed in the brain, has been shown recently to be required to maintain normal apoE levels and lipidation in the central nervous system. In addition, ABCA1 has been reported to modulate β-amyloid (Aβ) production *in vitro*. These observations raise the possibility that ABCA1 may play a role in the pathogenesis of Alzheimer disease. Here we report that the deficiency of ABCA1 does not affect soluble or guanidine-extractable Aβ levels in Tg-SwDI/B or amyloid precursor protein/presenilin 1 (APP/PS1) mice, but rather is associated with a dramatic reduction in soluble apoE levels in brain. Although this reduction in apoE was expected to reduce the amyloid burden *in vivo*, we observed that the parenchymal and vascular amyloid load was increased in Tg-SwDI/B animals and was not diminished in APP/PS1 mice. Furthermore, we observed an increase in the proportion of apoE retained in the insoluble fraction, particularly in the APP/PS1 model. These data suggested that ABCA1-mediated effects on apoE levels and lipidation influenced amyloidogenesis *in vivo*.

Alzheimer disease (AD)[8] is the most common cause of senile dementia and currently affects ~40% of the population over 80 years of age. Clinically, AD is characterized by severe impairments in memory and executive cortical functions as well as difficulties in language, calculation, visuospatial perception, behavior, and judgment (1). Characteristic

neuropathological hallmarks of AD include intraneuronal fibrillary tangles composed of hyperphosphorylated tau protein and amyloid deposits that are composed largely of Aβ peptides, apolipoprotein E (apoE), lipids, and other proteins that accumulate in the neural parenchyma and the cerebrovasculature (2, 3). Aβ peptides are a heterogeneous group of peptides 39–43 amino acids in length that are proteolytically cleaved from amyloid precursor protein (APP) by γ- and β-secretases (4, 5). Aβ40 and Aβ42 are the main Aβ species in the brain. Aβ42 is less soluble and is present in all types of senile plaques, whereas Aβ40 is the major species deposited in cerebral blood vessels (4–7).

Most affected individuals have late onset AD that typically manifests after 70 years of age. However, a number of families develop the disease in their 4th or 5th decades (8, 9). The cases of familial AD result from mutations within APP or secretase components (8, 10). For example, the Swedish mutation (K670M/N671L) increases the amount of Aβ peptide that is generated from APP (11, 12). Other APP mutations, including the Dutch (E693D) and Iowa (Q694N) mutations, alter the charge of the Aβ peptide and result in amyloid deposition predominantly in the cerebral blood vessels rather than in the parenchyma (13–16). In addition to mutations in APP, over 100 different mutations have been identified in presenilin-1 alone (17). However, less than 5% of the overall clinical burden of AD is caused by mutations in APP and presenilins combined.

To date, the only well established risk factor for late-onset AD is apoE (18, 19). In the human population, apoE exists as three major alleles (apoE2, apoE3, and apoE4), and inheritance of an apoE4 allele increases the risk of developing AD at an earlier age, whereas inheritance of apoE2 delays the age of onset of AD (20–22). How apoE functions in the pathogenesis of AD is a subject of intense investigation. ApoE is a component of several lipoprotein subclasses, including very low density lipoprotein and HDL particles in the peripheral circulation, where apoE acts to mediate their uptake by apoE receptors (23, 24). In the central nervous system, apoE is synthesized and secreted by astrocytes and microglia and serves as the major cholesterol carrier in the brain and cerebrospinal fluid (25–29). In the brain, apoE expression is increased under conditions of chronic or acute neuronal damage, where it is believed to acquire lipids from damaged neuronal processes and redeliver these lipids to neurons during reinnervation (30–33).

In addition to lipid trafficking, apoE also plays a major role in Aβ metabolism. ApoE binds avidly to Aβ peptides and is found within amyloid plaques (34, 35). ApoE is believed to play a major role in the conversion of Aβ peptides from soluble to fibrillar form, based on the observation that apoE-deficient animals are unable to form mature amyloid *in vivo* (36–40). Although Aβ is deposited in the brains of

[8] The abbreviations used are: AD, Alzheimer disease; Aβ, β-amyloid; apoE, apolipoprotein E; APP, amyloid precursor protein; PS1, presenilin 1; ELISA, enzyme-linked immunosorbent assay; GAPDH, glyceraldehyde-3-phosphate dehydrogenase; ANOVA, analysis of variance; PBS, phosphate-buffered saline; HDL, high density lipoprotein; LRP, receptor-related protein; F, female; M, male.

apoE-deficient mice, the deposits do not contain structural amyloid as defined by the ability to bind thioflavine or Congo Red dyes (36–40). Furthermore, amyloid deposition is similar in distribution but less extensive in apoE heterozygous mice, suggesting a dose-dependent effect of apoE level on amyloid formation (41). Therefore, factors that affect apoE abundance may also affect amyloid deposition and influence the onset or progression of AD.

The ATP-binding cassette transporter ABCA1 has recently been shown to modulate apoE levels in the brain, cerebrospinal fluid, and plasma (42, 43). In peripheral tissues, the primary biochemical function of ABCA1 is to transport cholesterol and phospholipids from the plasma membrane to lipid-free apoAI, a reaction that constitutes the first step in HDL biogenesis (44). The pre-β-HDL particles generated from this reaction circulate in the bloodstream and acquire additional lipids to form mature HDL particles. ABCA1-dependent lipid transport to apoAI is the major pathway by which excess sterols from peripheral tissues are transported to the liver where they are converted into bile acids and excreted from the body. Mutation of one *ABCA1* allele causes familial hypoalphalipoproteinemia, a mild disorder of peripheral lipid metabolism characterized by reduced plasma HDL levels (45). Mutation of both alleles of *ABCA1* results in Tangier disease, which is characterized by a nearly complete absence of plasma HDL, deposition of intracellular cholesterol esters, and an increased risk of cardiovascular disease (45–47).

In addition to high expression in liver and macrophages, ABCA1 is also abundant in the central nervous system (48–51). ABCA1 is expressed in neurons, astrocytes, and microglia and is transcriptionally induced by liver X receptor and retinoic X receptor agonists, similar to ABCA1 regulation in noncentral nervous system cells (48–51). Although the functions of ABCA1 in the brain are not completely understood, it is likely that ABCA1 participates in the regulation of lipid trafficking among the various cell types within the brain. We and others have shown that ABCA1 mediates cholesterol efflux to apoE and regulates the secretion of apoE from astrocytes and microglia (42, 43). Lack of ABCA1 results in accumulation of lipids in cultured glia, impaired secretion of glia-derived apoE, and a drastic reduction of apoE levels in the brain, particularly in the hippocampus and striatum (42, 43). Furthermore, ABCA1-deficient glia exhibit impaired cholesterol efflux to apoE (42), and the low level of apoE that remains in the cerebrospinal fluid and brains of ABCA1-deficient mice is poorly lipidated (43). The observation that ABCA1 is a critical modulator of apoE abundance and lipidation in the central nervous system raises the possibility that ABCA1 may influence the onset or progression of AD through its effects on apoE.

Many previous studies have shown that intracellular cholesterol levels modify the cleavage of APP by secretases (52–57). Low intracellular cholesterol favors the non-amyloidogenic cleavage of APP by α-secretase and leads to decreased Aβ generation, whereas high intracellular cholesterol favors APP cleavage by β- and γ-secretases and thereby increases Aβ production (52–57). *In vitro*, two recent studies showed that increased ABCA1 reduced the generation of Aβ peptides derived from human APP (51, 58), and a third study found that excess ABCA1 increased the generation of endogenous rodent Aβ (59). The lack of consensus among these studies underscores the need to evaluate the role of ABCA1 on Aβ levels in a physiologically relevant *in vivo* setting.

Recently, Koldamova *et al.* (60) demonstrated that Aβ40 and Aβ42 levels were significantly reduced in APP23 mice treated with the liver X receptor ligand TO901317, concomitant with increased ABCA1 expression in neurons. Although these results support a role for neuronal ABCA1 in Aβ production *in vivo*, TO901317 induces the expression of several other genes in addition to *ABCA1*. For example, TO901317 has been reported to stimulate the expression of apoE in glial cell lines and in mice (61), although other groups have not observed significant increases in apoE expression in response to TO901317 (60, 62). TO901317 also induces other members of the ABC-cassette transporter superfamily that may also participate in central nervous system lipid homeostasis.

Because ABCA1 is expressed in several cell types in the brain, ABCA1 may play multiple roles in the pathogenesis of AD. For example, neuronal ABCA1 may play a prominent role in regulating intraneuronal cholesterol content, thereby influencing the production of Aβ peptides. From this perspective, the deficiency of ABCA1 would be predicted to increase intraneuronal lipids and lead to elevated Aβ levels. On the other hand, glial ABCA1 is crucial for normal apoE levels and lipidation (42, 43). Because apoE is required for amyloid deposition (36–39), and deficiency of ABCA1 results in a 70% reduction in apoE levels, the absence of ABCA1 would be predicted to decrease amyloid deposition *in vivo*. Therefore, the lack of ABCA1 could theoretically result in opposite outcomes in amyloid deposition depending upon whether the major role of ABCA1 is on Aβ production or Aβ clearance and deposition via apoE. Determining whether deficiency of ABCA1 increases, decreases, or has no net effect on Aβ and amyloid burden will therefore require investigating the effect of ABCA1 deficiency on Aβ and amyloid deposition *in vivo* where the physiological interactions among neurons and glia during the process of amyloid deposition are preserved.

We therefore crossed ABCA1-deficient mice to two independent murine models of AD to determine the impact of ABCA1 on amyloid burden, Aβ levels, and apoE levels *in vivo*. Here we report that elimination of ABCA1 has no measurable impact on the steady-state levels of soluble or guanidine-extractable human Aβ when crossed to either model, and no effect on endogenous murine Aβ levels in the parental ABCA1-deficient mice. Lack of ABCA1 did result in the expected reduction in soluble apoE levels, consistent with previous results (42, 43). Because apoE is required for amyloid deposition, we expected that each model would exhibit fewer amyloid plaques in the absence of ABCA1. However, despite a large reduction in apoE levels, amyloid burden was not diminished in either model. Our results support the hypothesis that ABCA1 has minimal impact on Aβ levels *in vivo* but that ABCA1-mediated effects on lipidation and levels of apoE may participate in the conversion of Aβ from soluble peptides to insoluble amyloid.

EXPERIMENTAL PROCEDURES

Mouse Models—ABCA1-deficient mice were generously provided by Dr. Omar Francone (Pfizer Global Research and Development (Groton, CT)) and are on a DBA/1LacJ genetic background (63). Tg-SwDI/B mice express the human APP770 cDNA containing the Swedish (K670M/N671L), Dutch (E693Q), and Iowa (D694N) mutations and are on a congenic C57Bl/6 genetic background (64). Neuronally specific expression is directed from the mouse Thy1.2 promoter. Beginning at 24–30 weeks of age, thioflavine S-positive amyloid deposits are observed primarily within the cerebrovasculature, as the Dutch and Iowa mutations alter the charge of the Aβ peptide and promote deposition in cerebral microvessels rather than in the neural parenchyma (64). The APP/PS1 (line 85) mouse model (The Jackson Laboratories) co-expresses two transgenes that are each expressed from the mouse prion promoter. One transgene is a chimeric mouse/human APP650 cDNA containing the Swedish (K670M/N671L) mutations, and the other is the human presenilin 1 (PS1) gene containing the ΔE9 (deletion of exon 9) mutation (65). Both transgenes are inserted at a single locus and are inherited together. The level of transgenic APP expression in the

FIGURE 1. **Presence of the APP transgene does not modify ABCA1 abundance.** ABCA1 protein levels in the hippocampus of Tg-SwDI/B (*A*) and APP/PS1 (*B*) mice were determined by Western blot and quantitated by densitometry. *Graphs* are expressed as % of wild-type (APP−, ABCA1$^{+/+}$ mice were assigned 100%) and illustrate at least two independent experiments. *A,* data correspond to four individual mice per genotype (2F and 2M). *B,* data represent APP−, ABCA1$^{+/+}$ ($n = 5$ (3F and 2M); APP+, ABCA1$^{+/+}$ ($n = 5$ (2F and 3M)); APP−, ABCA1$^{+/-}$ ($n = 6$ (3F and 3M)); APP+, ABCA1$^{+/-}$ ($n = 6$ (2F and 4M)); APP−, ABCA1$^{-/-}$ ($n = 5$ (2F and 3M)); and APP+, ABCA1$^{-/-}$ ($n = 5$ (2F and 3M)). Western blots show two representative samples per group. GAPDH was used as an internal loading control. ** represents $p < 0.001$ compared with wild-type (APP-ABCA1$^{+/+}$) by ANOVA with Newman-Keuls post-test.
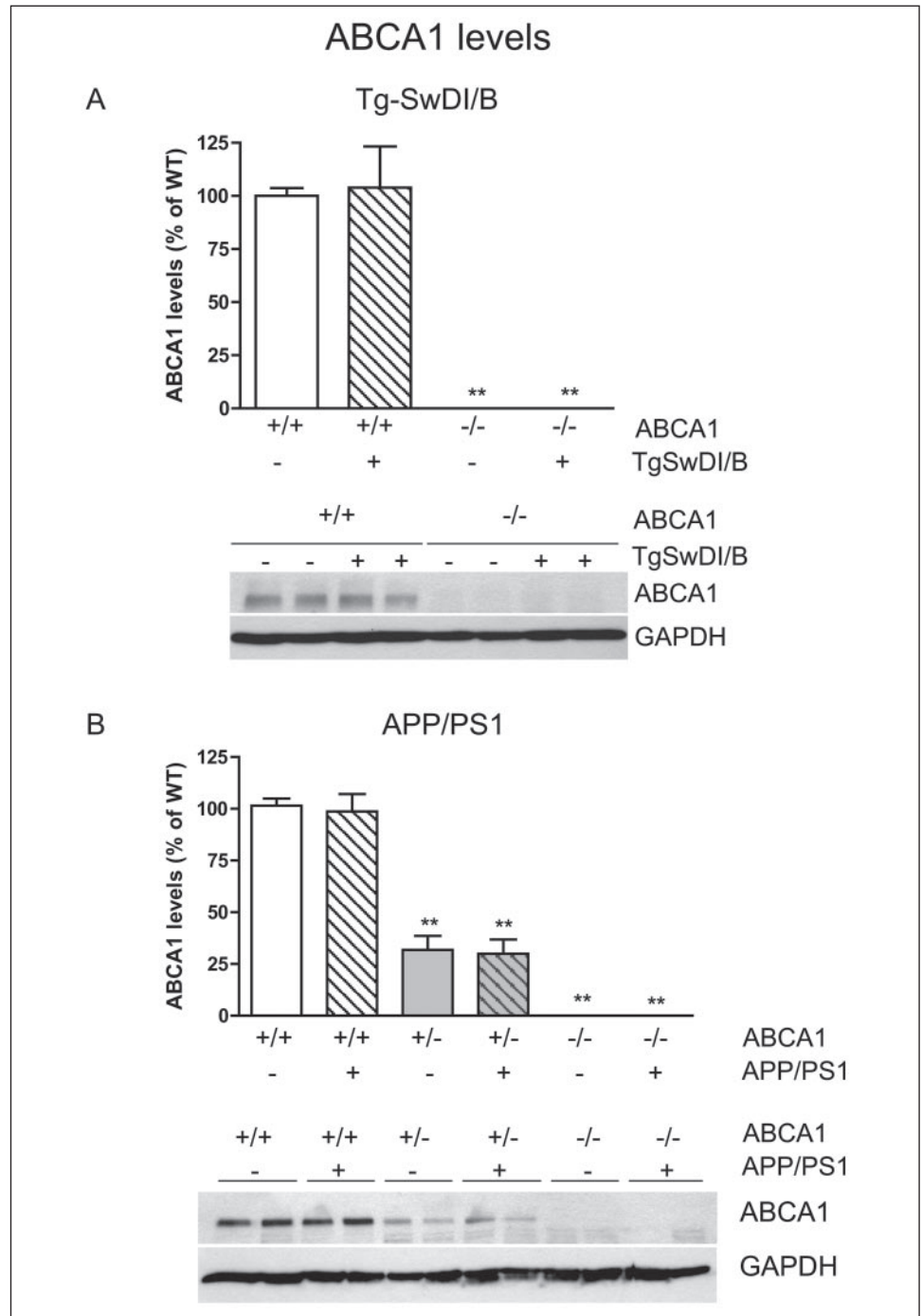
APP/PS1 mice is estimated to be ∼2–4-fold over murine APP levels (65). The APP/PS1 mice are maintained on a mixed F1 C3H/H3J × C57Bl/6 genetic background and develop parenchymal thioflavine S-positive amyloid deposits at ∼36–40 weeks of age (65). All animals were maintained on a standard chow diet (PMI LabDiet 5010, containing 24% protein, 5.1% fat, and 0.03% cholesterol). All procedures involving experimental animals were performed in accordance with protocols from the Canadian Council of Animal Care and the University of British Columbia Committee on Animal Care.

Tissue Collection—Mice were anesthetized with a mixture of 20 mg/kg xylazine (Bayer) and 150 mg/kg ketamine (Bimeda-MTC) and transcardially perfused with phosphate-buffered saline (PBS) for 7 min. Brains were removed and divided into right and left hemispheres. Cor-

tex and hippocampus were dissected from the right hemisphere and kept frozen at −80 °C until analysis. The left hemisphere was immersion-fixed in 10% neutral buffered formalin for at least 48 h and cryoprotected in 30% sucrose in PBS at 4 °C.

Protein Extraction from Brain Tissue—Protein extractions from cortical and hippocampal regions were done in three consecutive steps in order to evaluate apoE, ABCA1, APP, and Aβ levels from the same animals. Brain regions were homogenized in ∼8 volumes of ice-cold PBS containing Complete protease inhibitor (Roche Applied Science) in a Tissuemite homogenizer. The homogenate was centrifuged at 4 °C for 45 min at 12,500 rpm in a microcentrifuge (Eppendorf). The supernatant (soluble fraction) was removed and used to evaluate soluble apoE. No ABCA1 or APP was detectable in this fraction, as both are mem-

brane-bound proteins. The pellets from the PBS solubilization step were then resuspended in ice-cold lysis buffer (containing 10% glycerol, 1% Triton X-100, and Complete protease inhibitor (Roche Applied Science) in PBS) and centrifuged at 4 °C for 10 min at 9,000 rpm in order to extract ABCA1 and APP. The pellet from this step (insoluble fraction) was finally solubilized in 5 M guanidine hydrochloride in 50 mM Tris-HCl, pH 8.0, at room temperature for about 2.5–3 h with continuous rotation in order to evaluate plaque-associated Aβ and apoE. Brain tissue from all animals was extracted in the identical manner, and all fractions were immediately frozen at −80 °C until analysis. Protein concentrations were determined by DC Protein Assay (Bio-Rad).

Western Blotting—ApoE, ABCA1, and APP levels were determined by Western blot. For soluble apoE (PBS fraction), ABCA1, and APP (lysis buffer fractions), protein concentrations were determined by DC protein assay (Bio-Rad) prior to analysis. Equal amounts of protein were electrophoresed through 10% SDS-polyacrylamide gels, electrophoretically transferred to polyvinylidene fluoride membrane (Millipore), and immunodetected using a murine-specific apoE antibody (Santa Cruz Biotechnology), a monoclonal anti-ABCA1 antibody raised against the second nucleotide binding domain (48), 22C11, which detects both murine and human APP (Chemicon), or an anti-GAPDH antibody (Chemicon) as a loading control. Blots were developed using enhanced chemiluminescence (Amersham Biosciences) according to the manufacturer's recommendations. For insoluble apoE, protein loading was normalized by Coomassie Blue staining of duplicate gels. Bands were quantitated by densitometry using NIH Image J software.

Aβ Measurements—Human Aβ levels were quantified by ELISA (BIOSOURCE) according to the manufacturer's protocol. Samples were analyzed diluted in reaction buffer as described in the manufacturer's protocol. Endogenous murine Aβ40 levels were quantified using 75 μg of protein from total hippocampal homogenates. The coating antibody used was R163 (66, 67) for Aβ40 (a generous gift from Dr. P. D. Mehta, New York Institute for Basic Research, Staten Island, NY). Plates were coated overnight at 4 °C and then blocked with PBS containing 0.1% bovine serum albumin for 2 h at room temperature. Following five washes with TBS-T (Tris-buffered saline containing 0.1% Tween 20), samples were incubated for 2 h at room temperature with biotinylated 4G8 (Signet Laboratories Inc., Dedham, MA) for 1 h at room temperature with agitation. The plates were washed five times, and streptavidin-alkaline phosphatase complex was added for 1 h at room temperature. Plates were finally washed five times with TBS-T and once with water, and AttoPhos reagent (Calbiochem) was added for 30–60 min, and a reading was taken on a Bio-Tek FL600 fluorescence microplate reader. Human and murine Aβ levels were normalized to total protein as measured by DC Protein Assay (Bio-Rad).

Histological Analysis—25-μm-thick, coronal sections were cut on fixed brains using a cryostat from the genu of the corpus callosum to the most caudal hippocampus. For thioflavine S staining, sections were immersed for 10 min in 1% thioflavine S solution followed by washing and dehydration in increasing ethanol concentrations from 70 to 100% followed by xylene. Slides were mounted in dibutyl phthalate xylene mounting medium (DBH) and visualized within the following 24 h. Aβ immunohistochemistry was performed as reported previously (68) with slight modifications. Briefly, floating sections were incubated in 88% formic acid for 5 min, incubated for 30 min with 0.3% H_2O_2 in PBS-T (0.01 M PBS, pH 7.4, containing 0.3% Triton X-100), transferred into 1% horse serum (Vector Laboratories) in PBS-T for 30 min, and incubated overnight at 4 °C in 1.5% horse serum in PBS-T containing antibodies 4G8 and 6E10 (Chemicon) (1:1000 dilution each) against residues 17–24 and 1–17 of Aβ, respectively. Sections were then washed with
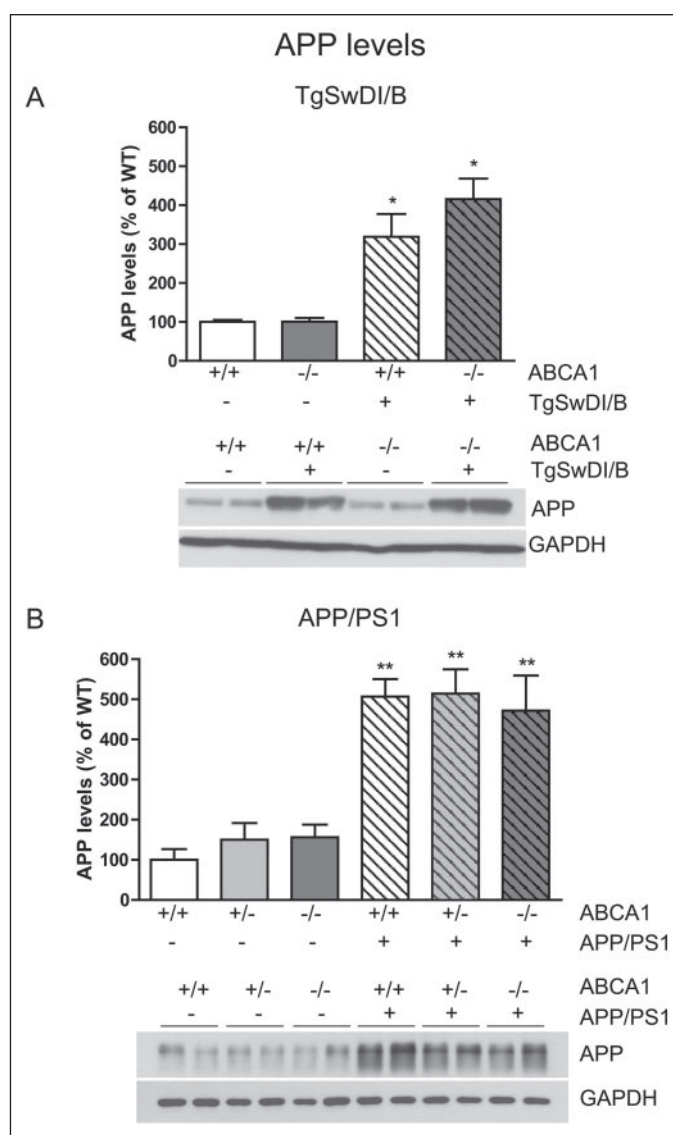

FIGURE 2. **APP levels are unaffected in the absence of ABCA1.** APP protein levels in hippocampus of Tg-SwDI/B mice (*A*) and cortex of APP/PS1 mice (*B*) were determined by Western blot and quantitated by densitometry. *Graphs* are expressed as % of wild-type (APP−, ABCA1$^{+/+}$ mice were assigned 100%) and illustrate at least two independent experiments. *A*, data correspond to four individual mice per genotype (2F and 2M). *B*, data represent four individual mice per genotype (2F and 2M). Western blots show two representative samples per group. GAPDH was used as an internal loading control. * represents $p < 0.01$ and ** represents $p < 0.001$ compared with wild-type (APP−, ABCA1$^{+/+}$) by ANOVA with Newman-Keuls post-test.

PBS-T, treated for 1 h at room temperature with a biotinylated anti-mouse antibody (1:1000, Vector Laboratories), and followed by incubation in avidin-biotinylated horseradish peroxidase complex (ABC Elite, Vector Laboratories; 1:1000) for 1 h at room temperature. Peroxidase labeling was visualized by incubation in 0.05% 3,3-diaminobenzidine (Sigma) and 0.001% H_2O_2 in 0.05 M Tris-HCl buffer, pH 7.6. After a 2-min incubation period, sections were washed, mounted on glass slides, and coverslipped with dibutyl phthalate xylene mounting medium. Imaging was performed on a Zeiss Axioplan 2 microscope using Metamorph capture software.

Quantitative Analysis of Amyloid and Aβ Burden—Amyloid load was quantitated in different brain regions depending on the mouse model. For the hippocampus (Tg-SwDI/B and APP/PS1), six sections, 300 μm apart and spanning the entire length of the hippocampus, were chosen for staining and subsequent analysis. For the thalamus (Tg-SwDI/B),
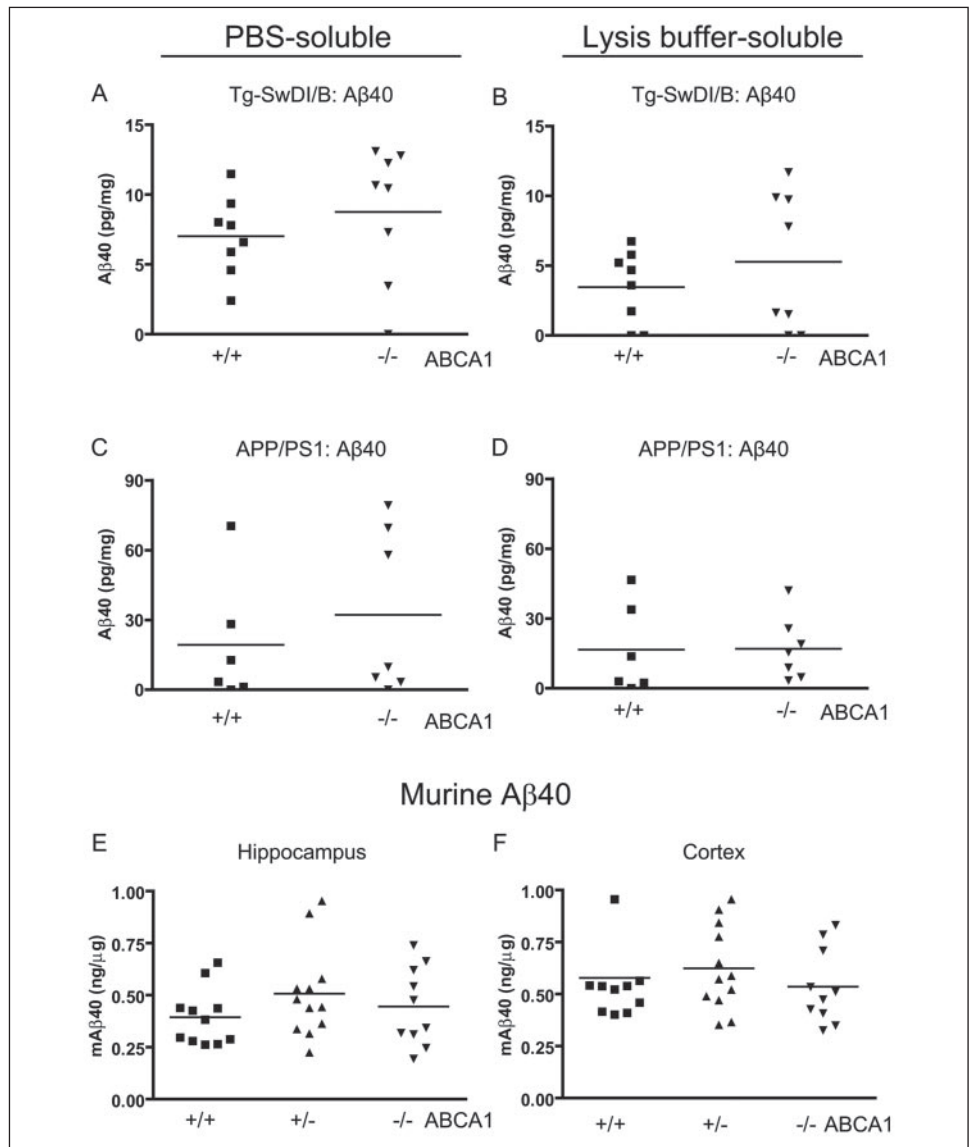
FIGURE 3. **Soluble Aβ levels are not affected by lack of ABCA1.** Soluble Aβ40 levels in Tg-SwDI/B hippocampi were quantitated from PBS (*A*) and lysis buffer (*B*) extracts. Soluble Aβ40 levels in APP/PS1 cortex were quantitated from the PBS (*C*) and lysis buffer (*D*) extracts. ELISA values were normalized to total protein as determined by DC protein assay. *Graphs* correspond to Tg-SwDI/B+, ABCA1$^{+/+}$ (*n* = 8 (4F and 4M) and Tg-SwDI/B+, ABCA1$^{-/-}$ (*n* = 8 (4F and 4M)) (*A* and *B*) and to APP+, ABCA1$^{+/+}$ (*n* = 6 (2F and 4M)) and APP+, ABCA1$^{-/-}$ (*n* = 7 (3F and 4M)) (*C* and *D*). Endogenous murine Aβ40 levels in hippocampus (*E*) and cortex (*F*) were determined by ELISA in ABCA1$^{+/+}$ (*n* = 11 (6F and 5M)), ABCA1$^{+/-}$ (*n* = 12 (6F and 6M)), and ABCA1$^{-/-}$ (*n* = 10 (6F and 4M)) mice. Values were normalized to total protein.

four sections, 300 μm apart, starting at the most rostral aspect of the thalamus were chosen. Quantification of amyloid in the cingulate cortex (APP/PS1) was performed on sections before the emergence of the genu of the corpus callosum on a total four sections, 300 μm apart. This systematic sampling strategy was chosen to account for subregional variations of hippocampal size and potential subregional variations in plaque burden. The slides were viewed in a Zeiss Axioplan 2 microscope under light of wavelength 450–490 nm. Colored images were captured using Metamorph software and a Cool Snap HQ camera (Photometrics). Camera settings were adjusted at the start of the experiment and maintained for uniformity. Using Metamorph software, low magnification (×2.5) images were acquired. A computer-generated grid composed of 16 higher magnification (×10) fields was superimposed on each ×2.5 image. Throughout the hippocampus, 50% of the ×10 fields was randomly selected, and images of these fields were acquired for analysis. Areas of the regions of interest in each ×10 image were outlined manually. The plaque/amyloid area within the fields of interest was identified by color and intensity-level threshold, the level of which was maintained throughout the experiment. After manual editing of staining artifacts, the thresholded and total areas, the amyloid load defined as (sum of thioflavine S staining area measured/sum of field area

analyzed) × 100 was calculated for each mouse. Images were quantitated by raters blinded to genotype.

For Aβ load, stained sections were chosen using the same sampling method using sections cut immediately before or after those stained with thioflavine S. Gray scale images were captured and analyzed as above. The Aβ load was defined as the (sum of Aβ immunoreactive area measured/sum of field area analyzed) × 100 and was determined by raters blinded to genotype.

The number of thioflavine S +ve plaques per unit area was also calculated for hippocampus and a larger cortical area in the APP/PS1 mice. For this procedure, plaques visible on 2.5x images were counted manually by raters blinded to genotype. The boundaries of the hippocampus were used, whereas limits of the larger cortical area were determined by transecting each image with a horizontal line through the corpus callosum and counting all thioflavine S positive plaques above this line. Plaque count totals were averaged between two independent raters blinded for genotype, corrected for total area, and expressed as the number of thioflavine S +ve plaques/μm^2.

Statistical Analysis—Data are shown as means ± S.E. One-way ANOVA with a Newman-Keuls post-test or two-tailed unpaired Student's *t* tests were used for statistical analysis. In the *t* test analyses,
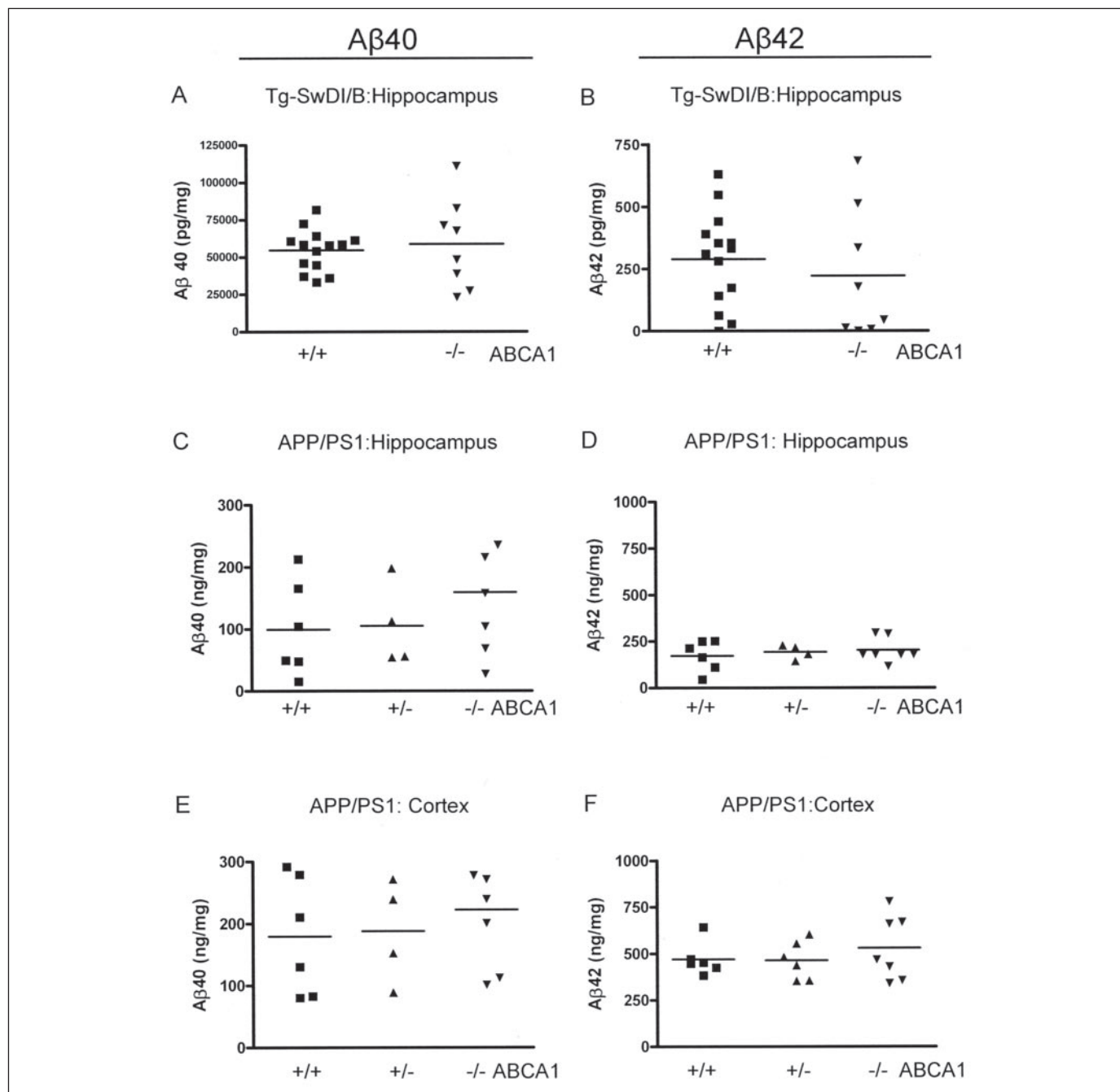
FIGURE 4. **Guanidine-extractable Aβ levels are independent of ABCA1 genotype.** Aβ40 and Aβ42 levels in hippocampus of Tg-SwDI/B (*A* and *B,* respectively) and in hippocampus (*C* and *D*) and cortex (*E* and *F*) of APP/PS1 mice were measured by ELISA. Values were normalized to total protein as determined by DC protein assay. *Graphs* correspond to Tg-SwDI/B+, ABCA1$^{+/+}$ ($n = 14$ (8F and 6M) and Tg-SwDI/B+, ABCA1$^{-/-}$ ($n = 8$ (4F and 4M)) (*A* and *B*) and to APP+, ABCA1$^{+/+}$ ($n = 6$ (2F and 4M)), APP+, ABCA1$^{+/-}$ ($n = $ at least 4 (2F and 2M)), and APP+, ABCA1$^{-/-}$ ($n = 7$ (3F and 4M)) (*C*–*F*).

Welch's correction for unequal variances was applied when variances were significantly different between groups. All statistical analyses were performed using Graphpad Prism (version 4.0; Graphpad software for Science Inc., San Diego).

RESULTS

ABCA1 Levels Are Unaffected by the APP and PS1 Transgenes—To evaluate whether the presence of an APP or PS1 transgene affected ABCA1 expression, we first determined ABCA1 protein levels in the hippocampus and cortex in two mouse models of AD. Tg-SwDI/B mice express human APP containing the Dutch (E693Q) and Iowa (D694N)

mutations in neurons under the control of the mouse Thy1 promoter (64). APP/PS1 mice use the murine prion promoter to co-express a chimeric mouse/human APP650 cDNA containing the Swedish (K670M/N671L) mutations, as well as the human PS1 gene containing the ΔE9 mutation (65). Tg-SwDI/B animals were examined at 10 months of age and contained abundant ABCA1 protein in wild-type mice and no detectable ABCA1 in ABCA1$^{-/-}$ mice (Fig. 1*A*). No effect of the APP transgene on ABCA1 levels was observed (Fig. 1*A*). APP/PS1 mice were examined at 12 months of age. As expected, ABCA1 levels were undetectable in the hippocampus of ABCA1$^{-/-}$ mice and were reduced by ~60% in ABCA1$^{+/-}$ mice compared with wild-type con-

TABLE ONE

Aβ levels, Aβ immunoreactivity, and amyloid load by region and mouse model in the presence or absence of ABCA1

	Hippocampus						Cortex					
	Wild type			ABCA1$^{-/-}$				Wild type			ABCA1$^{-/-}$		
	Mean	S.D.	n	Mean	S.D.	n	p value	Mean	S.D.	n	Mean	S.D.	n	p value
TgSwDI/B													
Aβ40 (pg/mg)	54626	13991	14	58701	29958	8	NS[a]	ND[b]			ND		
Aβ42 (pg/mg)	288.9	189	14	221.9	262.8	8	NS	ND			ND		
Aβ load (%)	0.1	0.063	8	0.26	0.169	8	<0.05	ND			ND		
Amyloid load (%)	0.076	0.058	8	0.255	0.125	8	<0.005	ND			ND		
APP/PS1													
Aβ40 (ng/mg)	99.25	76.74	6	159.3	99.11	7	NS	179.2	94.87	6	222.5	91.66	7	NS
Aβ42 (ng/mg)	172.7	82.4	6	203	65.95	7	NS	470.2	89.6	6	529.7	172.8	7	NS
Aβ load (%)	1.56	0.97	4	0.79	0.38	5	NS	ND			ND		
Amyloid load (%)	0.62	0.35	6	0.73	0.44	7	NS	1.16	0.55	6	0.99	0.26	7	NS
Plaque no. (plaques/μm^2)	1.71e-05	1.00e-05	6	2.54e-05	1.33e-05	7	NS	4.21e-05	1.65e-05	6	4.74e-05	5.74e-06	7	NS
Parental ABCA1$-/-$													
Aβ40 (ng/μg)	0.394	0.137	11	0.445	0.189	10	NS	0.577	0.208	11	0.535	0.179	10	NS

[a] NS indicates not significant.
[b] ND indicates not determined.

trols irrespective of the presence of the APP or PS1 transgenes (Fig. 1*B*). Similar results were observed in the cortex of APP/PS1 mice (data not shown).

Deficiency of ABCA1 Does Not Affect APP or Aβ Levels in Vivo—Western blots of brain lysates were then used to determine whether deficiency of ABCA1 affected APP expression *in vivo*. As expected, total APP levels were significantly higher in lysates of transgenic Tg-SwDI/B (Fig. 2*A*) and APP/PS1 (Fig. 2*B*) brains compared with nontransgenic controls. APP protein levels were identical in wild-type, heterozygous, and ABCA1-deficient mice in both Tg-SwDI/B and APP/PS1 models (Fig. 2, *A* and *B*), demonstrating that ABCA1 does not influence APP abundance. In contrast to the reported 50% increase in APP levels over endogenous levels in the Tg-SwDI/B model (64), we observed that transgenic mice expressed 2–3-fold more APP than controls in our cohorts. Possible explanations for this discrepancy include different protein extraction protocols and the different genetic background of the animals upon breeding to ABCA1 hemizygous mice.

Because ABCA1 has been reported previously to either increase (59) or decrease (51, 58) Aβ production in cultured cells, we next evaluated whether ABCA1 affected the steady-state levels of human Aβ in the brains of Tg-SwDI/B and APP/PS1 mice with various *ABCA1* gene doses. Several serial extraction protocols have been developed to remove different Aβ pools from brain tissue. We developed an extraction protocol to allow the levels of Aβ to be determined from the same brain samples that were used to measure ABCA1, APP, and apoE protein levels. Brains were first extracted in PBS and then in lysis buffer, and soluble and weakly membrane-associated Aβ was measured from each fraction. No significant differences in Aβ40 levels were observed in either fraction from either model (Fig. 3, *A–D*). PBS-soluble and lysis buffer-soluble Aβ42 levels were below the detection limit of our assay (data not shown). We also evaluated the impact of ABCA1 deficiency on steady-state levels of endogenous murine Aβ40 in the parental ABCA1-deficient mice, and we found that murine Aβ40 levels were indistinguishable among wild-type, heterozygous, and ABCA1-deficient mice in the cortex and hippocampus (Fig. 3, *E* and *F*). These results demonstrate that the abundance of soluble Aβ species is not elevated in the absence of ABCA1.

To facilitate comparison of insoluble Aβ levels in our studies to several other relevant publications (39, 69, 70), we elected to use 5 M guanidine to extract Aβ that is likely to be strongly associated with membranes or deposited within plaques. No significant differences were observed in steady-state guanidine-extractable Aβ40 or Aβ42 levels in either model (Fig. 4). These data are summarized in TABLE ONE and suggest that deletion of ABCA1 has no significant impact on either transgenic or endogenous steady-state Aβ levels *in vivo*.

ABCA1 Deficiency Increases Aβ Deposition in Tg-SwDI/B Mice—To evaluate the pattern and quantity of Aβ deposits, hemicoronal sections of Tg-SwDI/B and APP/PS1 brains were stained for Aβ deposits as described. In 10-month-old Tg-SwDI/B mice, there was a significant 2-fold increase in Aβ immunoreactivity in the absence of ABCA1 compared with controls (TABLE ONE), and the staining distribution pattern was indistinguishable between groups (Fig. 5). Most Aβ immunoreactivity in the hippocampus was observed in the subiculum and the polymorph layer of the dentate gyrus (Fig. 5*A*). In 12-month-old APP/PS1 mice, no significant differences in the distribution pattern or quantity of Aβ deposits were noted in the hippocampus of ABCA1-deficient animals compared with wild-type littermate controls (Fig. 5*B* and TABLE ONE). Deposits were observed throughout the hippocampus and cortex of APP/PS1 animals.

Deficiency of ABCA1 Reduces Soluble ApoE Levels in Vivo—We and others have shown previously that ABCA1 is required to maintain normal levels of apoE in the central nervous system (42, 43). Western blots were used to determine whether PBS-extractable apoE levels were decreased as expected in the presence of the APP or PS1 transgenes. In 10-month-old Tg-SwDI/B mice, PBS-soluble apoE levels were reduced by ~75% in APP+/ABCA1$^{-/-}$ hippocampus compared with APP+/ABCA1$^{+/+}$ controls ($p < 0.001$; Fig. 6*A*). Similarly, in 12-month-old APP/PS1 mice, soluble apoE levels were 80% lower in the hippocampus of mice lacking ABCA1 compared with animals with wild-type levels of ABCA1 (Fig. 6*B*). Mice with heterozygous levels of ABCA1 had normal levels of soluble apoE (Fig. 6*B*). Similar results were observed in the cortex of APP/PS1 mice (data not shown). These observations confirm our previous results and demonstrate that the influence of ABCA1 on apoE levels in brain is maintained in the presence of the APP and PS1 transgenes.

ApoE levels have been reported to be elevated in response to chronic or acute neuronal damage (30–33). We observed elevated levels of soluble apoE in APP/PS1 transgenic mice compared with
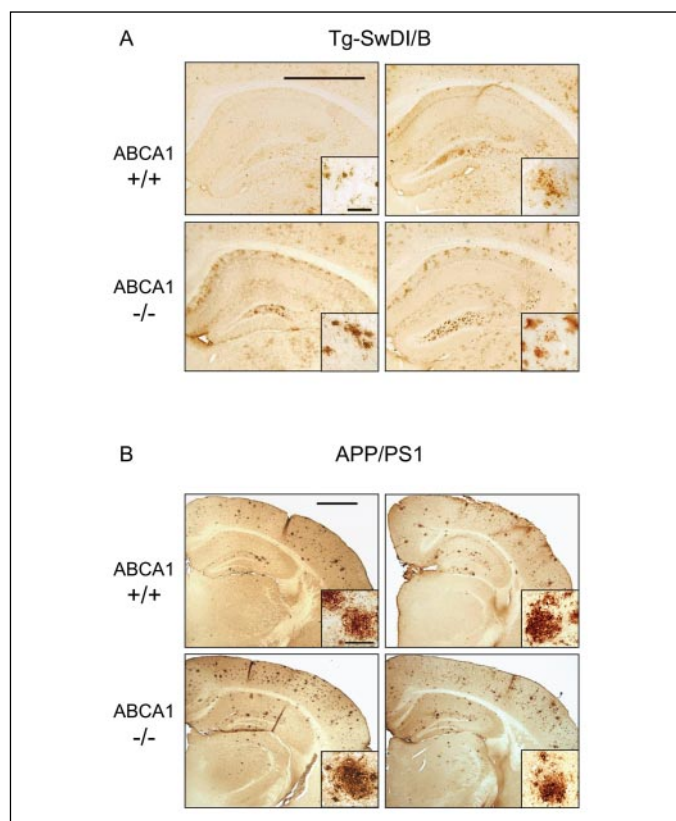
FIGURE 5. **Absence of ABCA1 does not alter Aβ distribution and elevates Aβ load in Tg-SwDI/B mice.** Immunohistochemistry for Aβ was performed as described in Tg-SwDI/B+, ABCA1$^{+/+}$ ($n = 8$ (4F and 4M)) and Tg-SwDI/B+, ABCA1$^{-/-}$ ($n = 8$ (4F and 4M)) (*A*) and in APP+, ABCA1$^{+/+}$ ($n = 4$ (1F and 3M)), APP+, ABCA1$^{+/-}$ ($n = 5$ (2F and 3M)), and APP+, ABCA1$^{-/-}$ ($n = 5$ (2F and 3M)) (*B*) brains. Pictures correspond to two representative mice per genotype at $\times 2.5$ magnification. *Insets* correspond to $\times 40$ magnification of individual plaques. *A, scale bars* represent 1000 μm (large hippocampal image) and 40 μm (*inset*). *B, scale bars* represent 1000 μm (large image) and 60 μm (*inset*).

nontransgenic controls that contained at least one functional copy of *ABCA1* (Fig. 6*B*), but we did not observe this effect in Tg-SwDI/B transgenic mice (Fig. 6*A*). This could be due to differences in the degree of AD pathology in each model at the time of assessment, including less amyloid deposition in Tg-SwDI/B compared with APP/PS1 mice and different distribution of amyloid, with thioflavine S +ve deposits being mostly parenchymal in the APP/PS1 and vascular in the Tg-SwDI/B animals.

In the APP/PS1 model with extensive Aβ deposition, APP/PS1 transgenic mice with wild-type levels of ABCA1 showed a significant increase in PBS-extractable apoE in the hippocampus (90%, $p < 0.001$) compared with ABCA1$^{+/+}$ mice lacking the APP/PS1 transgenes (Fig. 6*B*). ABCA1 heterozygous mice carrying the APP/PS1 transgenes also showed a trend toward increased apoE levels in the hippocampus (30%, $p > 0.05$) compared with ABCA1$^{+/-}$ mice lacking the APP and PS1 transgenes (Fig. 6*B*). Similar results were observed in the cortex of APP/PS1 mice (data not shown). These observations suggest that apoE expression is induced in mice with abundant Aβ deposition, consistent with a role for apoE in mitigating neuronal damage. Notably, apoE failed to be induced in the absence of ABCA1 in either model, suggesting that ABCA1 is required to observe the increase in apoE secretion under conditions of neuronal stress.

Deficiency of ABCA1 Increases Amyloid Deposition in Tg-SwDI/B Mice—In both Tg-SwDI/B and APP/PS1 models, guanidine-extractable Aβ levels were unchanged in the absence of ABCA1, suggesting that
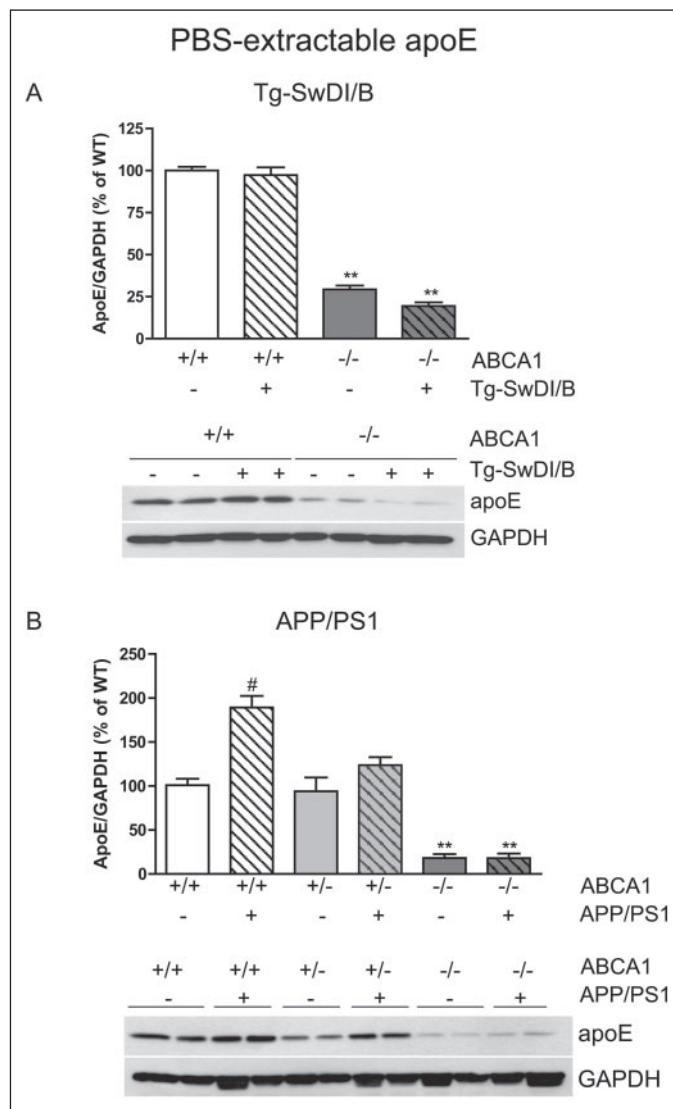

FIGURE 6. **ABCA1 deficiency decreases soluble apoE levels in cortex and hippocampus.** PBS-extractable apoE levels were determined by Western blot in hippocampus of Tg-SwDI/B (*A*) and APP/PS1 (*B*) mice and quantitated by densitometry. *Graphs* are expressed as % of wild-type (APP-ABCA1$^{+/+}$ mice were assigned 100%) and illustrate at least two independent experiments. *A*, data correspond to eight individual mice for each genotype (4F and 4M). *B*, data represent APP−, ABCA1$^{+/+}$ ($n = 6$ (3F and 3M)), APP+, ABCA1$^{+/+}$ ($n = 5$ (2F and 3M)), APP−, ABCA1$^{+/-}$ ($n = 6$ (3F and 3M)), APP+, ABCA1$^{+/-}$ ($n = 6$ (2F and 4M)), APP−, ABCA1$^{-/-}$ ($n = 4$ (2F and 2M)), and APP+, ABCA1$^{-/-}$ ($n = 5$ (2F and 3M)) mice. Western blots show two representative samples per group. GAPDH was used as an internal loading control. ** represents $p < 0.001$ compared with wild-type (APP−, ABCA1$^{+/+}$) control and # represents $p < 0.001$ compared with nontransgenic animals by ANOVA with Newman-Keuls post-test.

ABCA1 has minimal impact on the steady-state levels of Aβ. Furthermore, both models exhibited a robust decrease in soluble apoE levels. Based on these observations, we expected to observe less amyloid deposition in ABCA1-deficient mice, consistent with previous observations that the level of apoE is a key determinant of amyloid deposition in murine models (36, 71). However, contrary to our expectations of reduced amyloid burden, quantitative stereological assessment of amyloid in the hippocampus of 10-month-old Tg-SwDI/B mice revealed a significant 2-fold increase of amyloid in the absence of ABCA1, particularly in the subiculum and polymorph layer of the dentate gyrus ($p = 0.02$) (Fig. 7*A* and TABLE ONE). Deposits in the subiculum were observed to be mostly vascular, whereas the deposits in the dentate gyrus were predominantly parenchymal. These observations are con-
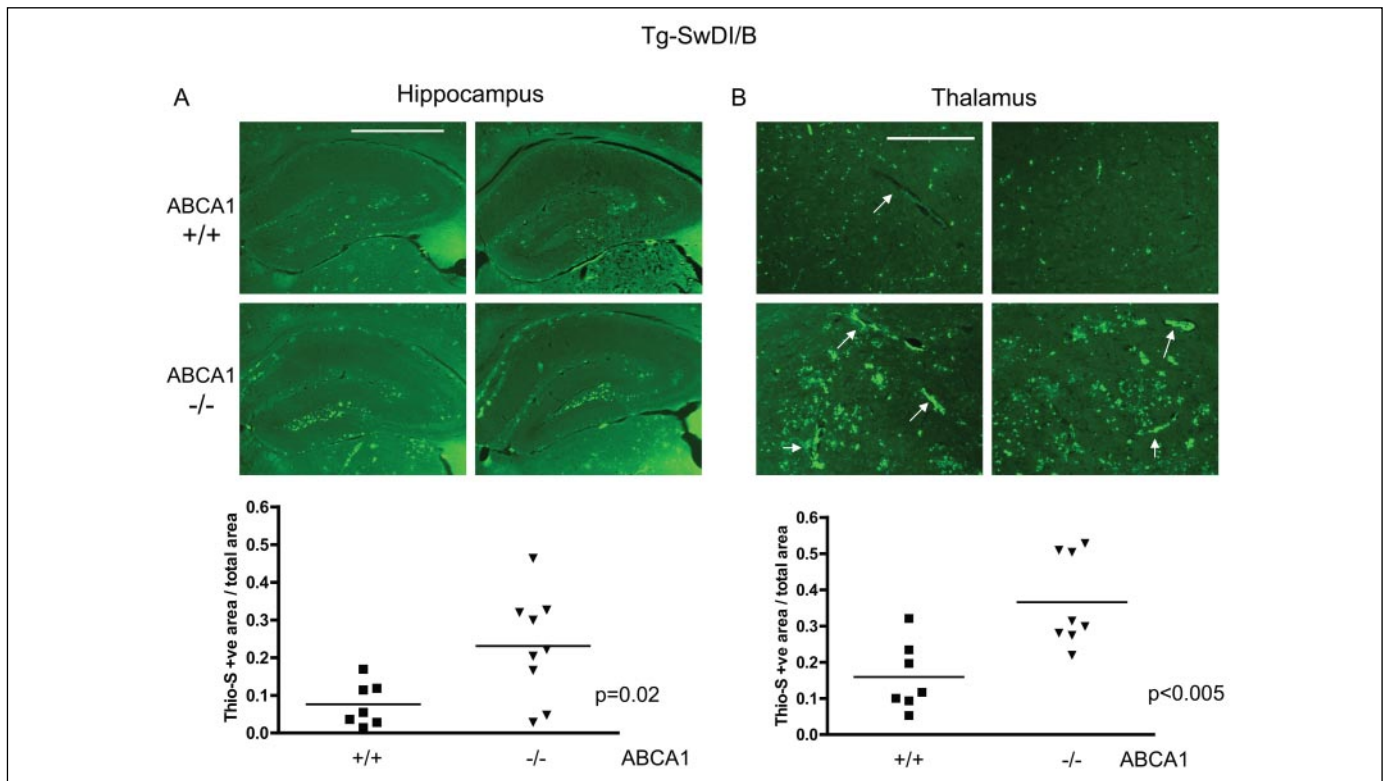
FIGURE 7. **Absence of ABCA1 increases amyloid deposition in Tg-SwDI/B mice.** Thioflavine S staining of hemicoronal sections from Tg-SwDI/B hippocampus (*A*) and thalamus (*B*) in the presence and absence of ABCA1. Pictures show two individual mice per genotype and correspond to ×2.5 images for the hippocampus (*A*) and ×10 images for thalamus (*B*). *Scale bars* represent 1000 μm in *A* and 250 μm in *B*. *Arrows* point toward vessels. Amyloid load was quantitated as described under "Experimental Procedures" in Tg-SwDI/B+, ABCA1$^{+/+}$ ($n = 7$ (3F and 4M)) and Tg-SwDI/B+, ABCA1$^{-/-}$ ($n = 8$ (4F and 4M)) mice. Student's *t* test was used for statistical analysis.

sistent with an increase in deposited Aβ in Tg-SwDI/B mice that lack ABCA1. We also examined the impact of ABCA1 on amyloid deposits in the thalamus, which is a heavily vascularized region. Thalamic amyloid deposits were also significantly increased by 2-fold in the absence of ABCA1 ($p < 0.005$; Fig. 7*B*). Vascular deposits involved larger vessels in ABCA1 deficient mice compared with wild-type controls.

Amyloid Burden Is Not Diminished Despite Reduced ApoE Levels in APP/PS1 Mice—Amyloid deposition was also assessed in the hippocampus and cortex of APP/PS1 mice between 12 and 13 months of age, a time in disease progression characterized by abundant amyloid deposits in this model. Again, contrary to our expectations of reduced amyloid due to lower apoE levels, amyloid burden was not significantly diminished in either the hippocampus (Fig. 8, *A* and *B*, and TABLE ONE) or cortex (Fig. 8, *C* and *D*, and TABLE ONE) of wild-type, heterozygous, and ABCA1-deficient mice. These findings are consistent with no significant change in Aβ deposits in APP/PS1 mice that lack ABCA1. However, unlike the Tg-SwDI/B model, we observed that deletion of ABCA1 resulted in no significant increase in amyloid burden or distribution in APP/PS1 mice when quantitated either by fluorescence threshold per area (Fig. 8 and TABLE ONE) or by plaque number per unit area (TABLE ONE).

ABCA1 Regulates ApoE Solubility in Brain—Previous studies have shown that insoluble, non-PBS-extractable apoE appears in transgenic AD mice during the development of amyloid plaques (72), suggesting that apoE becomes sequestered within plaques and is removed from the soluble pool. To determine whether the absence of ABCA1 affected this insoluble pool of apoE, we analyzed the guanidine-extractable pool of apoE by Western blot.

In Tg-SwDI/B mice, guanidine-soluble apoE levels were reduced only by 50% in the hippocampus of ABCA1-deficient mice compared with

mice with wild-type levels of ABCA1 ($p < 0.01$; Fig. 9). Because deficiency of ABCA1 resulted in a 75% reduction in soluble apoE levels, these observations suggest apoE may be beginning to be sequestered in amyloid plaques at this stage in pathogenesis.

In APP/PS1 mice with abundant plaques, we observed a clear ABCA1 dose-dependent increase in insoluble apoE levels in both hippocampus and cortex (Fig. 10). Compared with mice with wild-type levels of ABCA1, insoluble apoE was elevated by 63% ($p > 0.05$) in the hippocampus and by 175% ($p > 0.05$) in the cortex in ABCA1$^{+/-}$ compared with ABCA1$^{+/+}$ mice (Fig. 10, *A* and *B*, respectively). This increase in insoluble apoE was even more dramatic in the complete absence of ABCA1 (Fig. 10, *A* and *B*), with a 2-fold increase observed in both the hippocampus and cortex ($p < 0.01$).

These observations demonstrate that ABCA1 has a marked effect on the distribution of apoE in the brain. In the Tg-SwDI/B model, the lack of ABCA1 decreases the proportion of insoluble apoE in parallel with the decrease in soluble apoE. However, the decrease in the insoluble fraction of apoE is less than expected. In the APP/PS1 model, lack of ABCA1 results in a dramatic increase in the proportion of apoE found in the insoluble fraction. This observation suggests that absence of ABCA1 shifts the distribution of apoE from soluble to insoluble pools during the formation of amyloid plaques *in vivo*.

DISCUSSION

Much of the current research supports a role for cholesterol in AD (19, 73), suggesting that genes that regulate cholesterol metabolism may influence the pathogenesis of AD. The cholesterol and phospholipid transporter ABCA1 is a critical regulator of HDL metabolism in peripheral tissues, and is expressed in the brain where it has been shown recently to regulate apoE levels (42, 43). ABCA1 has also been impli-
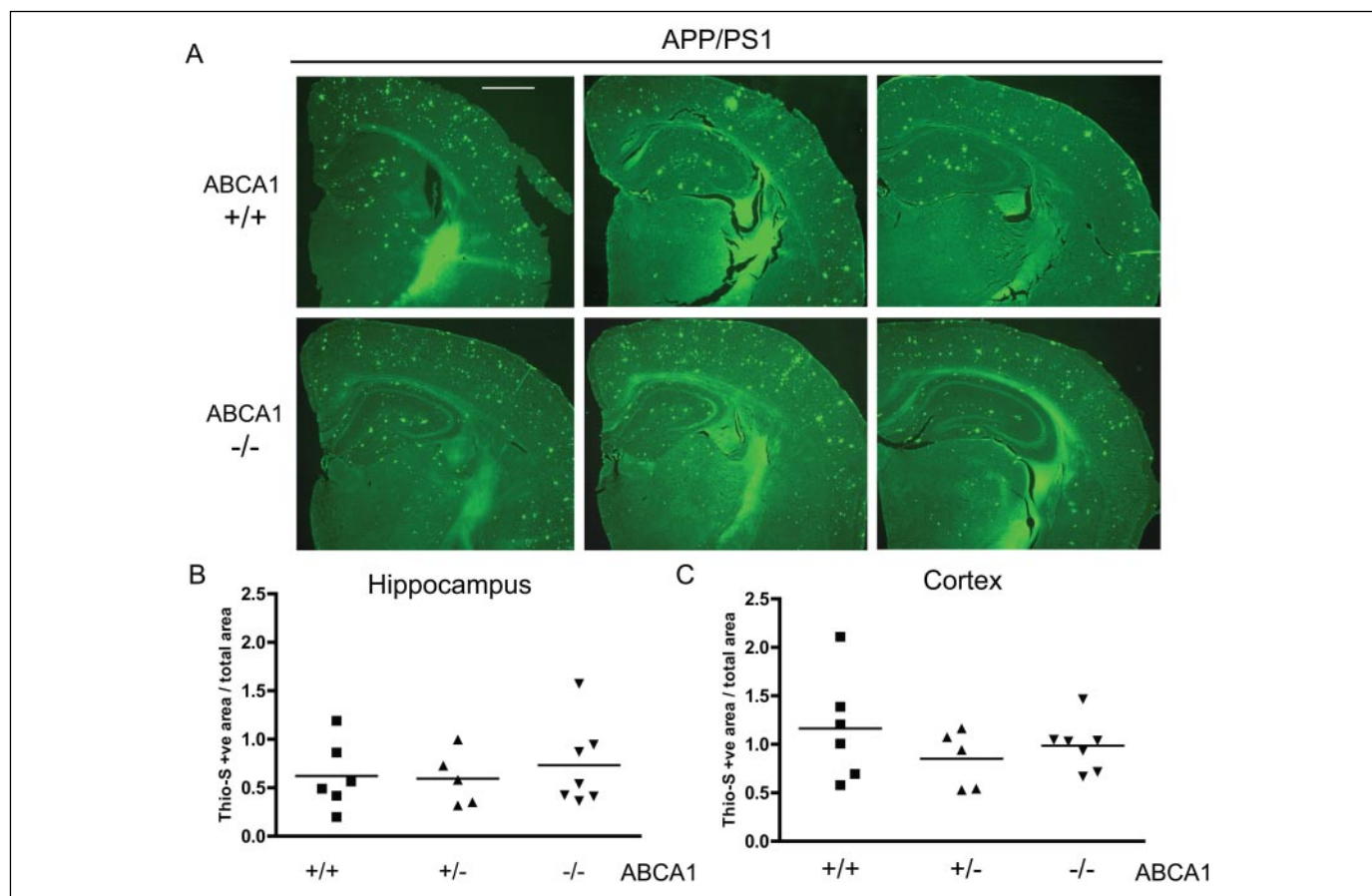
FIGURE 8. **Absence of ABCA1 does not diminish amyloid burden in APP/PS1 mice.** *A*, thioflavine S staining of hemicoronal sections from APP/PS1 mice in the presence and absence of ABCA1. *Scale bars* represent 1000 μm. *B*, amyloid load was quantitated in the hippocampus (*B*) and cingulate cortex (*C*) as described under "Experimental Procedures." The *graph* corresponds to APP/PS1+, ABCA1$^{+/+}$ ($n = 6$ (2F and 4M)), APP/PS1+, ABCA1$^{+/-}$ ($n = 5$ (2F and 3M)), and APP/PS1+, ABCA1$^{-/-}$ ($n = 7$ (3F and 4M)) mice. No significant differences were found by ANOVA.

cated in Aβ metabolism, and genetic studies suggest that polymorphisms in *ABCA1* may be associated with AD (74–76). These observations indicate that *ABCA1* may be a gene of interest for AD, although whether ABCA1 influences AD neuropathology *in vivo* and whether this occurs through effects on Aβ or apoE metabolism have not yet been addressed. We and Koldamova *et al.* (92) and Wahrle *et al.* (93) now report *in vivo* studies supporting a prominent role for ABCA1 in amyloidogenesis.

In this study, we investigated the impact of ABCA1 deficiency on steady-state Aβ levels, amyloid burden, and apoE abundance and distribution in the Tg-SwDI/B and APP/PS1 murine models of AD. Three major conclusions can be drawn from our study. First, the absence of ABCA1 did not significantly affect the levels of soluble or insoluble Aβ when crossed to either Tg-SwDI/B or APP/PS1 mice, nor did it alter the levels of endogenous murine Aβ in the parental ABCA1-deficient animals. These observations suggest that ABCA1 may not play a major role in Aβ production *in vivo*. Second, ABCA1 is required to maintain apoE levels *in vivo*. This was shown previously in the parental ABCA1$^{-/-}$ mice (42, 43) and is here confirmed upon breeding ABCA1-deficient mice to either the Tg-SwDI/B or APP/PS1 models. This observation suggests that the effect of glial ABCA1 on secretion of apoE from astrocytes and microglia remains similar across a variety of genetic backgrounds and in the presence of APP and PS1 transgenes. Third, and in contrast to our expectations, the ABCA1-mediated decrease of apoE levels failed to reduce amyloid and Aβ deposition in both the Tg-SwDI/B and APP/PS1 models. Based on the lack of effect of ABCA1

on Aβ levels but the pronounced effect of ABCA1 on apoE levels *in vivo*, we predicted amyloid deposition would be decreased in the absence of ABCA1, in line with previous observations that apoE levels determine the extent of amyloid deposition *in vivo* (36–39). In contrast, we observed more extensive parenchymal and vascular Aβ deposition and significantly elevated amyloid burden in the Tg-SwDI/B model despite a 75% reduction in apoE levels. In the APP/PS1 model, we again observed no decrease in amyloid burden despite an 80% decrease in soluble apoE levels in the absence of ABCA1.

One possible explanation for this relates to the role of apoE in Aβ clearance. Several studies have shown that apoE binds Aβ and suggested that this interaction might aid in the clearance of Aβ (77–80). Furthermore, two recent studies have shown that astrocytes are capable of clearing Aβ deposits from brain slices of aged APP transgenic mice (81, 82) and that this process is apoE-dependent (82). Together, these observations suggest that apoE is a key factor in regulating Aβ clearance *in vivo*. It is plausible to hypothesize that the low levels of apoE that exist in the brains of ABCA1-deficient mice are sufficient to allow for amyloid formation but are not enough to mediate effective Aβ clearance.

It is also possible that the poor lipidation of apoE in the absence of ABCA1 renders apoE prone to sequestration in amyloid plaques and enhances the conversion of Aβ from soluble peptides into amyloid. This hypothesis is supported by our observation that ABCA1 markedly affects the distribution of apoE in soluble compared with insoluble pools. In the Tg-SwDI/B model, ABCA1 deficiency reduced soluble apoE levels by 75% but reduced insoluble apoE levels only by 50% com-

FIGURE 9. **ABCA1-deficient Tg-SwDI/B mice have more insoluble apoE than expected.** Guanidine-soluble apoE levels were determined by Western blot in the hippocampus of Tg-SwDI/B−, ABCA1$^{+/+}$ ($n = 6$ (3F and 3M)), Tg-SwDI/B+, ABCA1$^{+/+}$ ($n = 9$ (5F and 4M)), Tg-SwDI/B−, ABCA1$^{-/-}$ ($n = 6$ (3F and 3M)), and Tg-SwDI/B+, ABCA1$^{+/-}$ ($n = 8$ (4F and 4M)) mice and quantitated by densitometry. Coomassie Blue staining of parallel gels was used to normalize for protein loading. *Graphs* are expressed as % of APP+, ABCA1$^{+/+}$ (these samples were assigned to 100%) and illustrate four independent experiments. Western blots show representative samples. [*] represents $p < 0.01$ compared with transgenic ABCA1 wild-type (APP+, ABCA1$^{+/+}$) control by ANOVA with Newman-Keuls post-test.
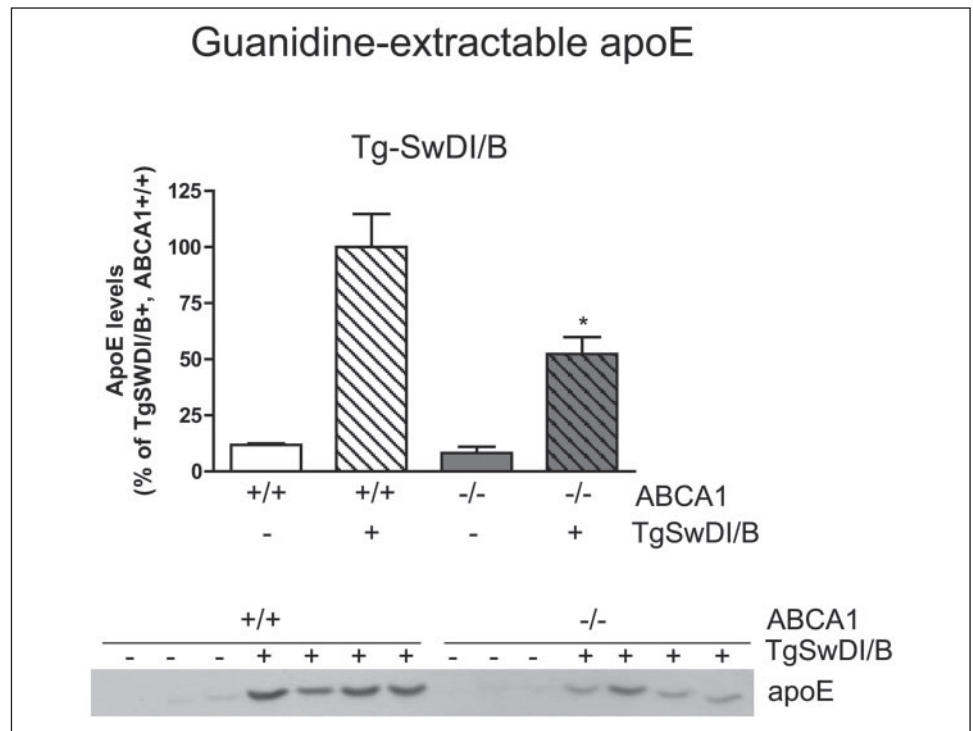
pared with mice with ABCA1. In the APP/PS1 model, soluble apoE was decreased by 80%, but apoE extracted from the insoluble fraction was elevated 2-fold in ABCA1$^{-/-}$ compared with ABCA1$^{+/+}$ mice. Wahrle *et al.* (93) also observed increased levels of guanidine-extractable insoluble apoE in transgenic PDAPP mice.

One limitation of our study is that the Western blot methodology used in our experiments does not allow us to quantitate accurately the relative proportion of insoluble compared with soluble apoE. Furthermore, the two AD models used in this study cannot be directly compared, due primarily to differences in the stage of disease pathogenesis and Aβ properties. Although the Tg-SwDI/B and APP/PS1 mice were examined at similar ages, the APP/PS1 model exhibited a 10-fold greater amyloid burden at the time of analysis compared with the Tg-SwDI/B animals. Additionally, Tg-SwDI/B mice express a human Aβ carrying the Dutch and Iowa mutations that may affect APP processing and influence the mechanism of Aβ deposition, whereas the APP/PS1 model generates wild-type human Aβ. These important differences in Aβ species in these two models could potentially alter binding to and deposition/clearance with apoE. Nevertheless, our observation that nearly all detectable apoE was present in the insoluble fraction in the APP/PS1 model raises the possibility that apoE continues to be recruited to amyloid plaques after they are seeded, and that the poorly lipidated apoE present in the brains of ABCA1$^{-/-}$ mice may either be recruited more effectively to amyloid deposits or is unable to clear these deposits as efficiently as normally lipidated apoE.

One of the strengths of this study is that we used two independent models of AD with different transgenes, promoters, and genetic backgrounds. The conclusions that the deficiency of ABCA1 has no effect on soluble or guanidine-extractable steady-state Aβ levels but significantly decreases apoE levels and fails to diminish amyloid burden are consistent in both these models, despite the important differences in Aβ species generated in the Tg-SwDI/B compared with APP/PS1 mice. Our major conclusions that deficiency of ABCA1 is associated with low levels of apoE, a shift in the distribution of apoE from soluble to insoluble pools, and either no change or increased deposition of fibrillar Aβ are

also similar to those of Koldamova *et al.* (92) and Wahrle *et al.* (93). By using APP23 mice, Koldamova *et al.* (92) report that the absence of ABCA1 results in significantly decreased apoE levels, significantly increased formic acid-extractable Aβ levels, and significantly increased parenchymal and vascular amyloid deposition. By using the PDAPP model, Wahrle *et al.* (93) observed that deficiency of ABCA1 leads to significantly elevated guanidine-extractable Aβ levels, a trend toward increased parenchymal and vascular deposition of Aβ and apoE, and a dramatic shift of apoE distribution from the soluble to the guanidine-extractable fraction. Taken together, three laboratories have now independently demonstrated that amyloid deposition fails to be reduced in four models of AD despite low apoE levels in the absence of ABCA1, and that these effects extend across differences in the transgene expressed, the mutations it carries, the promoter used, and the genetic background of the animals.

One difference among the three studies is in the effect of ABCA1 on Aβ levels. Koldamova *et al.* (92) found that lack of ABCA1 led to a trend toward increased soluble Aβ and a significant elevation of insoluble Aβ extracted using formic acid. Similarly, Wahrle *et al.* (93) report that the levels of soluble and guanidine-extractable Aβ are elevated in the absence of ABCA1. By using a different human-specific ELISA, we observed no differences in either soluble or guanidine-extractable Aβ levels between ABCA1-deficient and wild-type brains from either the Tg-SwDI/B or APP/PS1 models. It is possible that the guanidine extraction protocol used in our study may have failed to quantitatively extract some of the highly aggregated Aβ sequestered in plaques compared with formic acid extracts (83). Additionally, compared with the wild-type human Aβ generated in the APP/PS1 model, the mutations present in the Aβ of Tg-SwDI/B mice might interfere with its detection by ELISA, lowering the sensitivity of the test and obscuring possible increases in the insoluble fraction of Aβ. Differences in Aβ detection properties might also help to explain why we observed more deposited Aβ using immunohistochemistry in ABCA1-deficient Tg-SwDI/B mice compared with controls, yet did not detect elevated Aβ levels by ELISA.

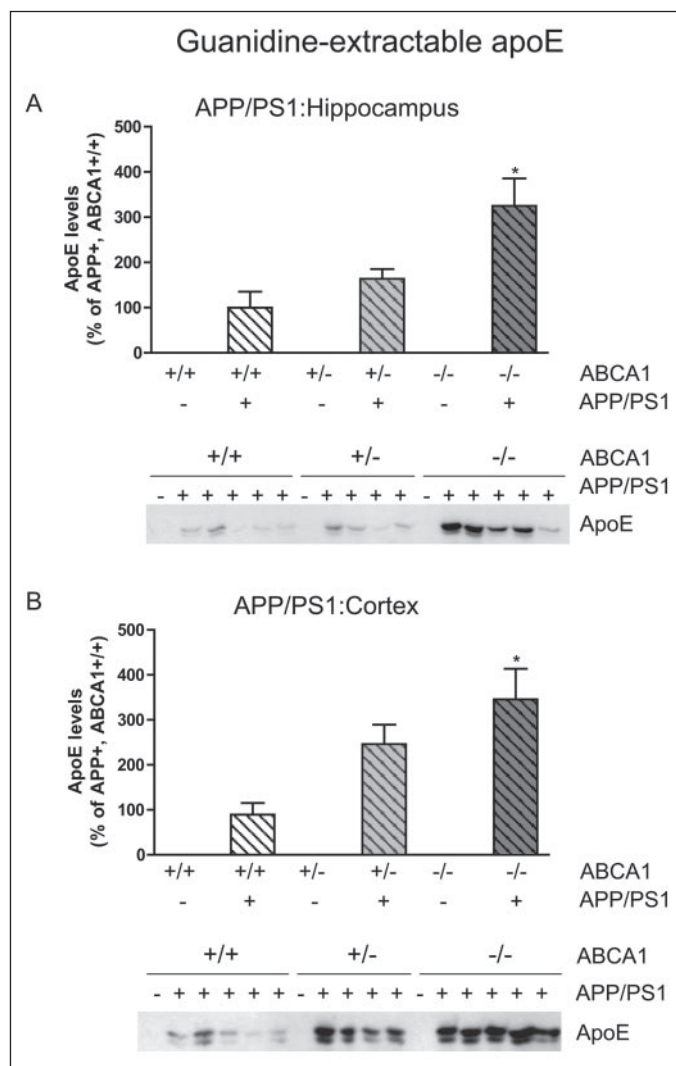A second difference among the studies relates to the proportion of

FIGURE 10. **Insoluble apoE levels are increased in APP/PS1 ABCA1-deficient mice.** Guanidine-soluble apoE levels were determined by Western blot in the hippocampus (*A*) and cortex (*B*) of APP−, ABCA1$^{+/+}$ (*n* = 2 (1F and 1M)), APP+, ABCA1$^{+/+}$ (*n* = 5 (2F and 3M)), APP−, ABCA1$^{+/-}$ (*n* = 2 (1F and 1M)), APP+, ABCA1$^{+/-}$ (*n* = 4 (2F and 2M)), APP−, ABCA1$^{-/-}$ (*n* = 3 (1F and 2M)), and APP+, ABCA1$^{-/-}$ (*n* = 5 (2F and 3M)) mice and quantitated by densitometry. Coomassie Blue staining of parallel gels was used to normalize for protein loading. *Graphs* are expressed as % of APP+, ABCA1$^{+/+}$ (these samples were assigned to 100%) and illustrate at least two independent experiments. Western blots show representative samples. * represents *p* < 0.01 compared with transgenic ABCA1 wild-type (APP+, ABCA1$^{+/+}$) control by ANOVA with Newman-Keuls post-test.

apoE residing in the soluble or insoluble fractions. Koldamova *et al.* (92) did not detect elevated levels of insoluble apoE after formic acid extraction, whereas we and Wahrle *et al.* (93) both observed accumulation of apoE in the guanidine-extractable fraction. Furthermore, Wahrle *et al.* (93) demonstrated that this apoE co-localized with amyloid.

The mechanisms underlying the shift in apoE distribution in soluble to insoluble fractions remain to be elucidated. The low density lipoprotein receptors and low density lipoprotein receptor-related proteins are the major apoE receptors in the central nervous system (84–86), and LRP is postulated to mediate clearance of Aβ-apolipoprotein complexes (86). Because delipidated apoE binds LRP poorly (85, 87), and because the lipidation status of apoE also influences its interactions with Aβ (78, 89, 90), it is possible that that the poorly lipidated apoE that exists in the brains of ABCA1-deficient mice (42, 43) may interact differently with Aβ, and the resulting complexes may not be efficiently recognized by LRP. Together, these mechanisms could lead to delayed clearance and increased deposition of Aβ.

Given the large number of studies demonstrating that intracellular cholesterol levels influence APP processing, an alternative explanation of our results is that an increase in Aβ production mediated by cholesterol-enriched ABCA1-deficient neurons may be precisely balanced by diminished Aβ and amyloid deposition resulting from ABCA1-mediated reductions in apoE levels. Because we observed no change in Aβ levels in our study, we did not measure Aβ production directly by testing for changes in APP CTF levels. Notably, despite detecting an increase in Aβ levels, Aβ production was observed to be unaffected in the absence of ABCA1 in the APP23 and PDAPP models (92, 93). However, because our study, as well as those of Koldamova *et al.* (92) and Wahrle *et al.* (93), used total ABCA1-deficient mice, elucidating the *in vivo* impact of ABCA1 on Aβ production independently of its effect on glia-derived lipoprotein homeostasis will require additional investigations in neuronal and glia-specific ABCA1 knock-out mice.

Whether the prevalence of AD is increased in Tangier disease patients that lack ABCA1 has not been specifically addressed, primarily because Tangier disease is a rare disease and most patients do not survive past 70 years of age (91). To our knowledge, there is only one case report of a proband with a compound mutation in the *ABCA1* gene who developed and died of complications related to CAA (88). Three studies have investigated whether single nucleotide polymorphisms in the *ABCA1* gene are associated with AD (74–76). Wollmer *et al.* (74) reported that the R219K gain-of-function single nucleotide polymorphism in *ABCA1* (R219K) has been suggested to delay the age of onset of AD by 1.6 years. Katzov *et al.* (75) reported significant associations with the R219K, R1587K, and V771M on AD in single marker and haplotype analyses conducted on European subjects. However, these findings were not replicated in a large case-control study of North American subjects using either single marker or haplotype analyses (76). Further investigations will therefore be required to determine whether inactivation of ABCA1 affects AD in humans. Nevertheless, the results of our study, together with Koldamova *et al.* (92) and Wahrle *et al.* (93), suggest that the impact of ABCA1 on AD may largely be mediated through its effect on apoE levels and/or lipidation status.

REFERENCES

1. Price, D. L., Tanzi, R. E., Borchelt, D. R., and Sisodia, S. S. (1998) *Annu. Rev. Genet.* **32**, 461–493
2. Morris, J. C. (1996) *Acta Neurol. Scand.* **165**, (suppl.) 41–50
3. Geldmacher, D. S., and Whitehouse, P. J., Jr. (1997) *Neurology* **48**, S2–S9
4. Haass, C., and Selkoe, D. J. (1993) *Cell* **75**, 154–159
5. Selkoe, D. J. (2001) *Physiol. Rev.* **81**, 741–766
6. Blennow, K., and Hampel, H. (2003) *Lancet Neurol.* **2**, 605–613
7. Bales, K. R., Dodart, J. C., DeMattos, R. B., Holtzman, D. M., and Paul, S. M. (2002) *Mol. Interv.* **2**, 363–375
8. Sherrington, R., Rogaev, E., Liang, Y., Rogaeva, E., Levesque, G., Ikeda, M., Chi, H., Lin, C., Li, G., Holman, K., Tsuda, T., Mar, L., Foncin, J. F., Bruni, A. C., Montesi, M. P., Sorbi, S., Rainero, I., Pinessi, L., Nee, L., Chumakov, I., Pollen, D., Brookes, A., Sansosu, P., Polinsky, R. J., Wasco, W., Da Silva, H. A. R., Haines, J. L., Pericak-Vance, M., Tanzi, R., Roses, A. D., Fraser, P. E., Rommens, J. M., and St. George-Hyslop, P. (1995) *Nature* **375**, 754–760
9. Nishimura, M., Yu, G., and St. George-Hyslop, P. H. (1999) *Clin. Genet.* **55**, 219–225
10. Vassar, R., Bennett, B. D., Babu-Khan, S., Kahn, S., Mendiaz, E. A., Denis, P., Teplow, D. B., Ross, S., Amarante, P., Loeloff, R., Luo, Y., Fisher, S., Fuller, J., Edenson, S., Lile, J., Jarosinski, M. A., Biere, A. L., Curran, E., Burgess, T., Louis, J. C., Collins, F., Treanor, J., Rogers, G., and Citron, M. (1999) *Science* **286**, 735–741
11. Lake, S. (1991) *Lakartidningen* **88**, 1271–1272

12. Citron, M., Oltersdorf, T., Haass, C., McConlogue, L., Hung, A. Y., Seubert, P., Vigo-Pelfrey, C., Lieberburg, I., and Selkoe, D. J. (1992) *Nature* **360,** 672–674

13. Levy, E., Carman, M. D., Fernandez-Madrid, I. J., Power, M. D., Leiberbrug, I., van Duinen, S. G., Bots, G. T., Luyendijk, W., and Frangione, B. (1990) *Science* **248,** 1124–1126

14. Van Broeckhoven, C., Haan, J., Bakker, E., Hardy, J. A., Van Hul, W., Wehnert, A., Vegter van der Vlis, M., and Roos, R. A. (1990) *Science* **248,** 1120–1122

15. Grabowski, T. J., Cho, H. S., Vonsattel, J. P., Rebeck, G. W., and Greenberg, S. M. (2001) *Ann. Neurol.* **49,** 697–705

16. Miravalle, L., Tokuda, T., Chiarle, R., Giaccone, G., Bugiani, O., Tagliavini, F., Frangione, B., and Ghiso, J. (2000) *J. Biol. Chem.* **275,** 27110–27116

17. Selkoe, D. J. (2001) *Proc. Natl. Acad. Sci. U. S. A.* **98,** 11039–11041

18. Tanzi, R. E., and Bertram, L. (2001) *Neuron* **32,** 181–184

19. Wellington, C. L. (2004) *Clin. Genet.* **66,** 1–16

20. Poirier, J., Davignon, J., Bouthillier, D., Kogan, S., Bertrand, P., and Gauthier, S. (1993) *Lancet* **342,** 697–699

21. Corder, E. H., Saunders, A. M., Strittmatter, W. J., Schmechel, D. E., Gaskell, P. C., Small, G. W., Roses, A. D., Haines, J. L., and Pericak-Vance, M. A. (1993) *Science* **261,** 921–923

22. Corder, E. H., Saunders, A. M., Risch, N. J., Strittmatter, W. J., Schmechel, D. E., Gaskell, P. C., Rimmler, J. B., Locke, P. A., Conneally, P. M., Schmader, K. E., Small, G. W., Roses, A. D., Haines, J. L., and Pericak-Vance, M. A. (1994) *Nat. Genet.* **7,** 180–184

23. Mahley, R. W., and Rall, S. C., Jr. (2000) *Annu. Rev. Genom. Hum. Genet.* **1,** 507–537

24. Curtiss, L. K., and Boisvert, W. A. (2000) *Curr. Opin. Lipidol.* **11,** 243–251

25. Ladu, M. J., Reardon, C., Van Eldik, L., Fagan, A. M., Bu, G., Holtzmann, D., and Getz, G. S. (2000) *Ann. N. Y. Acad. Sci.* **903,** 167–175

26. Ladu, M. J., Gilligan, S. M., Lukens, J. R., Cabana, V. G., Reardon, C. A., Van Eldik, L. J., and Holtzman, D. A. (1998) *J. Neurochem.* **70,** 2070–2081

27. Koch, S., Donarski, N., Goetze, K., Kreckel, M., Sturernburg, H. J., Buhmann, C., and Beisiegel, U. (2001) *J. Lipid Res.* **42,** 1143–1151

28. Demeester, N., Castro, G., Desrumaux, C., De Geitere, C., Fruchart, J. C., Santens, P., Mulleners, E., Engelborghs, S., De Deyn, P. P., Vandekerckhove, J., Rosseneu, M., and Labeur, C. (2000) *J. Lipid Res.* **41,** 963–974

29. Danik, M., Champagne, D., Petit-Turcotte, C., Beffert, U., and Poirier, J. (1999) *Crit. Rev. Neurobiol.* **13,** 357–407

30. Poirier, J. (2000) *Ann. N. Y. Acad. Sci.* **924,** 81–90

31. Poirier, J. (1994) *Trends Neurosci.* **17,** 525–530

32. Ignatius, M. J., Gebicke-Harter, P. J., Pitas, R. E., and Shooter, E. M. (1987) *Prog. Brain Res.* **71,** 177–184

33. Ignatius, M. J., Gebicke-Harter, P. J., Skene, J. H., Schilling, J. W., and Weisgraber, K. H. (1986) *Proc. Natl. Acad. Sci. U. S. A.* **83,** 1125–1129

34. Atwood, C. S., Martins, R. N., Smith, M. A., and Perry, G. (2002) *Peptides (N. Y.)* **23,** 1343–1350

35. Burns, M. P., Noble, W. J., Olm, V., Gaynor, K., Casey, E., LaFrancois, J., Wang, L., and Duff, K. (2003) *Brain Res. Mol. Brain Res.* **110,** 119–125

36. Bales, K. R., Verina, T., Dodel, R., Du, Y., Alsteil, L., Bender, M., Hyslop, P., Johnstone, E. M., Little, S. P., Cummins, D. J., Piccardo, P., Ghetti, B., and Paul, S. M. (1997) *Nat. Genet.* **17,** 263–264

37. Bales, K. R., Verina, T., Cummins, D. J., Du, Y., Dodel, R. C., Saura, J., Fishman, C. E., DeLong, C. A., Piccardo, P., Petegnief, V., Ghetti, B., and Paul, S. M. (1999) *Proc. Natl. Acad. Sci. U. S. A.* **96,** 15233–15238

38. Irizarry, M. C., Rebeck, G. W., Cheung, B., Bales, K., Paul, S. M., Holzman, D., and Hyman, B. T. (2000) *Ann. N. Y. Acad. Sci.* **920,** 171–178

39. Fagan, A. M., Watson, M., Parsadanian, M., Bales, K. R., Paul, S. M., and Holtzman, D. M. (2002) *Neurobiol. Dis.* **9,** 305–318

40. Miao, J., Vitek, M. P., Xu, F., Previti, M. L., Davis, J., and Van Nostrand, W. E. (2005) *J. Neurosci.* **25,** 6271–6277

41. Holtzman, D. M., Fagan, A. M., Mackey, B., Tenkova, T., Sartorius, L., Paul, S. M., Bales, K., Ashe, K. H., Irizarry, M. C., and Hyman, B. T. (2000) *Ann. Neurol.* **47,** 739–747

42. Hirsch-Reinshagen, V., Zhou, S., Burgess, B. L., Bernier, L., McIsaac, S. A., Chan, J. Y., Tansley, G. H., Cohn, J. S., Hayden, M. R., and Wellington, C. L. (2004) *J. Biol. Chem.* **279,** 41197–41207

43. Wahrle, S. E., Jiang, H., Parsadanian, M., Legleiter, J., Han, X., Fryer, J. D., Kowalewski, T., and Holtzman, D. M. (2004) *J. Biol. Chem.* **279,** 40987–40993

44. Hayden, M. R., Clee, S. M., Brooks-Wilson, A., Genest, J., Jr., Attie, A., and Kastelein, J. J. P. (2000) *Curr. Opin. Lipidol.* **11,** 117–122

45. Brooks-Wilson, A., Marcil, M., Clee, S. M., Zhang, L., Roomp, K., van Dam, M., Yu, L., Brewer, C., Collins, J. A., Molhuizen, H. O. F., Loubser, O., Ouellette, B. F. F., Fichter, K., Ashbourne Excoffon, K. J. D., Sensen, C. W., Scherer, S., Mott, S., Denis, M., Martindale, D., Frohlich, J., Morgan, K., Koop, B., Pimstone, S. N., Kastelein, J. J. P., Genest, J., Jr., and Hayden, M. R. (1999) *Nat. Genet.* **22,** 336–345

46. Rust, S., Rosier, M., Funke, H., Amoura, Z., Piette, J.-C., Deleuze, J.-F., Brewer, H. B., Jr., Duverger, N., Denèfle, P., and Assmann, G. (1999) *Nat. Genet.* **22,** 352–355

47. Bodzioch, M., Orsó, E., Klucken, J., Langmann, T., Böttcher, A., Diederich, W., Drobnik, W., Barlage, S., Büchler, C., Porsch-Özcürümez, M., Kaminski, W. E., Hahmann, H. W., Oette, K., Rothe, G., Aslanidis, C., Lackner, K. J., and Schmitz, G. (1999) *Nat. Genet.* **22,** 347–351

48. Wellington, C. L., Walker, E. K., Suarez, A., Kwok, A., Bissada, N., Singaraja, R., Yang, Y.-Z., Zhang, L. H., James, E., Wilson, J. E., Francone, O., McManus, B. M., and Hayden, M. R. (2002) *Lab. Investig.* **82,** 273–283

49. Singaraja, R. R., Bocher, V., James, E. R., Clee, S. M., Zhang, L.-H., Leavitt, B. R., Tan, B., Brooks-Wilson, A., Kwok, A., Bissada, N., Yang, Y.-Z., Liu, G., Tafuri, S. R., Fievet, C., Wellington, C. L., Staels, B., and Hayden, M. R. (2001) *J. Biol. Chem.* **276,** 33969–33979

50. Lawn, R. M., Wade, D. P., Couse, T. L., and Wilcox, J. N. (2001) *Arterioscler. Thromb. Vasc. Biol.* **21,** 378–385

51. Koldamova, R. P., Lefterov, I. M., Ikonomovic, M. D., Skoko, J., Lefterov, P. I., Isanski, B. A., DeKosky, S. T., and Lazo, J. S. (2003) *J. Biol. Chem.* **278,** 13244–13256

52. Fassbender, K., Simons, M., Bergmann, C., Stroick, M., Lütjohann, D., Keller, P., Runz, H., Kühl, S., Bertsch, T., von Bergmann, K., Hennerici, M., Beyreuther, K., and Hartmann, T. (2001) *Proc. Natl. Acad. Sci. U. S. A.* **98,** 5856–5861

53. Kojro, E., Gimple, G., Lammich, S., März, W., and Fahrenholz, F. (2001) *Proc. Natl. Acad. Sci. U. S. A.* **98,** 5815–5820

54. Simons, M., Keller, P., De Strooper, B., Beyreuther, K., Dottie, C. G., and Simons, K. (1998) *Proc. Natl. Acad. Sci. U. S. A.* **95,** 6460–6464

55. Bodovitz, S., and Klein, W. L. (1996) *J. Biol. Chem.* **271,** 4440–4452

56. Buxbaum, J. D., Geoghagan, N. S., and Friedhoff, L. T. (2001) *J. Alzheimers Dis.* **3,** 221–229

57. Ehehalt, R., Keller, P., Haass, C., Thiele, C., and Simons, K. (2003) *J. Cell Biol.* **160,** 113–123

58. Sun, Y., Yao, J., Kim, T.-W., and Tall, A. R. (2003) *J. Biol. Chem.* **278,** 27688–27694

59. Fukumoto, H., Deng, A., Irizarry, M. C., Fitzgerald, M. L., and Rebeck, G. W. (2002) *J. Biol. Chem.* **277,** 48508–48513

60. Koldamova, R. P., Lefterov, I. M., Staufenbiel, M., Wolfe, D., Huang, S., Glorioso, J. C., Walter, M., Roth, M. G., and Lazo, J. S. (2005) *J. Biol. Chem.* **280,** 4079–4088

61. Liang, Y., Lin, S., Beyer, T. P., Zhang, Y., Wu, X., Bales, K. R., DeMattos, R. B., May, P. C., Li, S. D., Jiang, X. C., Eacho, P. I., Cao, G., and Paul, S. M. (2004) *J. Neurochem.* **88,** 623–634

62. Whitney, K. D., Watson, M. A., Collins, J. L., Benson, W. G., Stone, T. M., Numerick, M. J., Tippin, T. K., Wilson, J. G., Winegar, D. A., and Kliewer, S. A. (2002) *Mol. Endocrinol.* **16,** 1378–1385

63. McNeish, J., Aiello, R. J., Guyot, D., Turi, T., Gabel, C., Aldinger, C., Hoppe, K. L., Roach, M. L., Royer, L. J., de Wet, J., Broccardo, C., Chimini, G., and Francone, O. L. (2000) *Proc. Natl. Acad. Sci. U. S. A.* **97,** 4245–4250

64. Davis, J., Xu, F., Deane, R., Romanov, G., Previti, M. L., Zeigler, K., Zlokovic, B. V., and Van Nostrand, W. E. (2004) *J. Biol. Chem.* **279,** 20296–20306

65. Jankowsky, J. L., Fadale, D. J., Anderson, J., Xu, G. M., Gonzales, V., Jenkins, N. A., Copeland, N. G., Lee, M. K., Younkin, L. H., Wagner, S. L., Younkin, S. G., and Borchelt, D. R. (2003) *Hum. Mol. Genet.* **13,** 159–170

66. Vaucher, E., Aumont, N., Pearson, D., Rowe, W., Poirier, J., and Kar, S. (2001) *J. Chem. Neuroanat.* **21,** 323–329

67. Mehta, P. D., Pirttilä, T., Mehta, S. P., Sersen, E. A., Aisen, P. S., and Wisniewski, H. M. (2000) *Arch. Neurol.* **57,** 100–105

68. Schwab, C., Hosokawa, M., and McGeer, P. L. (2004) *Exp. Neurol.* **188,** 52–64

69. Holtzman, D. M., Bales, K. R., Tenkova, T., Fagan, A. M., Parsadanian, M., Sartorius, L. J., Mackey, B., Olney, J., McKeel, D., Wozniak, D., and Paul, S. M. (2000) *Proc. Natl. Acad. Sci. U. S. A.* **97,** 2892–2897

70. DeMattos, R. B., Cirrito, J. R., Parsadanian, M., May, P. C., O'Dell, M. A., Taylor, J. W., Harmony, J. A., Aronow, B. J., Bales, K. R., Paul, S. M., and Holtzman, D. M. (2004) *Neuron* **41,** 193–202

71. Holtzman, D. M., Bales, K. R., Wu, S., Bhat, P., Parsadanian, M., Fagan, A. M., Chang, L. K., Sun, Y., and Paul, S. M. (1999) *J. Clin. Investig.* **103,** R15–R21

72. Naidu, A., Catalano, R., Bales, K., Wu, S., Paul, S. M., and Cordell, B. (2001) *Neuroreport* **12,** 1265–1270

73. Puglielli, L., Tanzi, R. E., and Kovacs, D. M. (2003) *Nat. Neurosci.* **6,** 345–351

74. Wollmer, M. A., Streffer, J. R., Lutjohann, D., Tsolaki, M., Iakovidou, V., Hegi, T., Pasch, T., Jung, H. H., Bergmann, K., Nitsch, R. M., Hock, C., and Papassotiropoulos, A. (2003) *Neurobiol. Aging* **24,** 421–426

75. Katzov, H., Chalmers, K., Palmgren, J., Andreasen, N., Johansson, B., Cairns, N. J., Gatz, M., Wilcock, G. K., Love, S., Pedersen, N. L., Brookes, A. J., Blennow, K., Kehoe, P. G., and Prince, J. A. (2004) *Hum. Mut.* **23,** 358–367

76. Li, Y., Tacey, K., Doil, L., van Luchene, R., Garcia, V., Rowland, C., Schrodi, S., Leong, D., Lau, K., Catanese, J., Sninsky, J., Nowotny, P., Holmans, P., Hardy, J., Powell, J., Lovestone, S., Thal, L., Owen, M., Williams, J., Goate, A., and Grupe, A. (2004) *Neurosci. Lett.* **366,** 268–271

77. Strittmatter, W. J., Saunders, A. M., Schmechel, D., Pericak-Vance, M., Enghild, J., Salveson, G. S., and Roses, A. D. (1993) *Proc. Natl. Acad. Sci. U. S. A.* **90,** 1977–1981

78. Ladu, M. J., Falduto, M. T., Manelli, A. M., Reardon, C. A., Getz, G. S., and Frail, D. E.

ASBMB

(1994) *J. Biol. Chem.* **269,** 23403–23406

79. Yang, D. S., Smith, J. D., Zhou, Z., Gandy, S. E., and Martins, R. N. (1997) *J. Neurochem.* **68,** 721–725
80. Aleshkov, S., Abraham, C. R., and Zannis, V. I. (1997) *Biochemistry* **36,** 10571–10580
81. Wyss-Coray, T., Loike, J. D., Brionne, T. C., Lu, E., Anankov, R., Yan, F., Silverstein, S. C., and Husemann, J. (2003) *Nat. Med.* **9,** 453–457
82. Koistinaho, M., Lin, S., Wu, X., Esterman, M., Koger, D., Hanson, J., Higgs, R., Liu, F., Malkani, S., Bales, K. R., and Paul, S. M. (2004) *Nat. Med.* **10,** 719–726
83. Cheng, I. H., Palop, J. J., Esposito, L. A., Bien-Ly, N., Yan, F., and Mucke, L. (2004) *Nat. Med.* **10,** 1190–1192
84. Beffert, U., Stolt, P. C., and Herz, J. (2004) *J. Lipid Res.* **454,** 403–409
85. Narita, M., Holtzman, D. M., Fagan, A. M., Ladu, M. J., Yu, L., Han, X., Gross, R. W., Bu, G., and Schwartz, A. L. (2002) *J. Biochem.* (*Tokyo*) **132,** 743–749
86. Zerbinatti, C. V., and Bu, G. (2005) *Rev. Neurosci.* **16,** 123–135
87. Ruiz, J., Kouiavskaia, D., Migliorini, M., Robinson, S., Saenko, E. L., Gorlatova, N., Li, D., Lawrence, D., Hyman, B. T., Weisgraber, K. H., and Strickland, D. K. (2005) *J. Lipid Res.* **46,** 1721–1731
88. Hong, S. H., Rhyne, J., Zeller, K., and Miller, M. (2002) *Biochim. Biophys. Acta* **1587,** 60–64
89. Ladu, M. J., Pederson, T. M., Frail, D. E., Reardon, C. A., Getz, G. S., and Falduto, M. T. (1995) *J. Biol. Chem.* **270,** 9039–9042
90. Tokuda, T., Calero, M., Matsubara, E., Vidal, R., Kumar, A., Permanne, B., Zlokovic, B., Smith, J. D., Ladu, M. J., Rostagno, A., and Ghiso, J. (2000) *Biochem. J.* **348,** 359–365
91. Fredrickson, D. S., Altrocchi, P. H., Avioli, L. V., Goodman, D. W. S., and Goodman, H. C. (1961) *Ann. Intern. Med.* **55,** 1016–1031
92. Koldamova, R., Staufenbiel, M., and Lefterov, I. (2005) *J. Biol. Chem.* **280,** 43224–43235
93. Wahrle, S. E., Jiang, H., Parsadanian, M., Hartman, R. E., Bales, K. R., Paul, S. M., and Holtzman, D. M. (2005) *J. Biol. Chem.* **280,** 43236–43242